

A simultaneous solution procedure for fully coupled fluid flows with structural interactions

by

Sandra Rugonyi

Nuclear Engineer, Balseiro Institute, Argentina (1995)

Submitted to the Department of Mechanical Engineering
in partial fulfillment of the requirements for the degree of

Master of Science in Mechanical Engineering

at the

MASSACHUSETTS INSTITUTE OF TECHNOLOGY

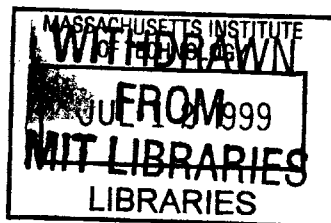
June 1999

© Massachusetts Institute of Technology 1999. All rights reserved.

Author
Department of Mechanical Engineering
May 19, 1999

Certified by
Klaus-Jürgen Bathe
Professor of Mechanical Engineering
Thesis Supervisor

Accepted by
Ain Ants Sonin
Chairman, Department Committee on Graduate Students



ENG



A simultaneous solution procedure for fully coupled fluid flows with structural interactions

by

Sandra Rugonyi

Submitted to the Department of Mechanical Engineering
on May 19, 1999, in partial fulfillment of the
requirements for the degree of
Master of Science in Mechanical Engineering

Abstract

A simultaneous solution algorithm to solve fully coupled fluid flow-structural interaction problems using finite element methods is proposed. The fluid is assumed to be a viscous (almost) incompressible medium modeled using the Navier-Stokes equations, whereas the structure is assumed to be a linear elastic isotropic solid undergoing small displacements. In addition, the structure is assumed to be very compliant and therefore the effects of the coupling onto the system response are expected to be important. The focus of this work is on the coupling procedure employed, the specific time integration schemes used in a transient analysis and on the efficiency of the solution procedure. Efficiency is realized by condensing out the internal structural degrees of freedom prior to the coupled solution analysis. The proposed time integration scheme is based on Gear's method, the Euler method or the trapezoidal rule for the fluid and the trapezoidal rule for the structure. A simplified analysis indicates unconditional stability (for the linearized system). Two example problems are solved to illustrate the applicability of the solution procedure.

Thesis Supervisor: Klaus-Jürgen Bathe
Title: Professor of Mechanical Engineering

Acknowledgments

First of all I would like to express my gratitude to Professor Klaus-Jürgen Bathe, my thesis advisor, for his constant support and wise suggestions in the development of my research work. I also want to thank Professor Eduardo Dvorkin who introduced me to the finite element procedures and encouraged me to continue my studies at MIT.

I would like to thank the people of the Finite Element Research Group at MIT (my office-mates) Daniel Pantuso, Ramon P. Silva, Alexander Iosilevich, Jean-François Hiller, Dena Hendriana and Suvranu De for their encouragement and support; and ADINA R & D for allowing me to use ADINA and for the help with the ADINA simulations presented here.

This research has been partially supported by the Rocca Fellowship for which I am very grateful.

My deepest gratitude goes to Mauro, my husband, whose encouragement, support and love mean the most to me.

Contents

1	Introduction	11
2	Governing equations	15
2.1	Kinematics of continuous media	15
2.1.1	Lagrangian formulation	17
2.1.2	Eulerian formulation	17
2.1.3	Arbitrary Lagrangian-Eulerian formulation	18
2.2	Lagrangian form of the conservation equations	19
2.2.1	Mass conservation	19
2.2.2	Momentum conservation	19
2.3	ALE form of the conservation equations	20
2.3.1	Mass conservation	20
2.3.2	Momentum conservation	22
2.4	Fluid flow equations	23
2.4.1	Compressible fluid	24
2.4.2	Incompressible fluid	25
2.4.3	Almost incompressible flow	25
2.5	Structural equations	26
2.5.1	Isotropic linear elastic material	26
2.6	Fluid flow-structural interface conditions	28
3	Finite element formulation	29
3.1	Fluid flow discretization	30

3.2	Structural equations	36
4	Coupling procedures for fluid flow-structural interaction problems	39
4.1	Coupling procedure	40
4.2	Different approaches for the solution of fluid-structure interaction problems	47
4.2.1	Simultaneous solution	47
4.2.2	Partitioned procedure	48
4.3	Proposed scheme	52
5	Stability analysis	55
5.1	Linearized fluid flow equations	56
5.2	Linear structural equations	58
5.3	Fluid-flow structural interaction equations	58
5.3.1	Partitioned procedures	59
5.3.2	Proposed scheme	59
6	Example solutions	67
6.1	Analysis of pressure wave propagation in a tube	67
6.2	Analysis of collapsible channel	72
7	Conclusions	79
A	Wave propagation in a compliant tube filled with fluid	82

List of Figures

2-1	Reference, spatial and mesh configurations.	16
3-1	9/3 element.	32
4-1	General fluid-structure interaction problem.	40
4-2	Finite element discretization of a fluid-structure interaction problem.	49
6-1	Pressure wave propagation problem. Geometry and boundary conditions considered.	68
6-2	Calculated pressure along the tube centerline for different instants of time, for the pressure wave propagation problem.	70
6-3	Deformation of tube and fluid velocities inside the tube due to pressure wave at $t = 0.01$ sec. Radius enlarged 10 times.	71
6-4	Collapsible channel problem. Geometry and boundary conditions considered.	73
6-5	Displacement history of mid-point of collapsible segment. Comparison between results obtained using the proposed scheme and ADINA. . .	75
6-6	Pressure (in Pa) and velocity distribution of the fluid inside the collapsible channel at $t=36.2$ sec.	76
6-7	Pressure (in Pa) and velocity distributions at maximum bulge out of collapsible segment (when the movement reaches the limit cycle) at $t = 62.7$ sec.	77

6-8	Pressure (in Pa) and velocity distributions at maximum inward deflection of the collapsible segment (when the movement reaches the limit cycle) at $t = 61.7$ sec.	78
-----	--	----

Chapter 1

Introduction

Finite element methods have been developed and extensively used for the analysis of structural and fluid problems. Although there are still major improvements desired in the formulation of finite element procedures for both fluids and structures (in particular for fluid flows at high Reynolds numbers and structures with highly nonlinear behavior) considerable research focus is now on new areas of application.

The availability of faster computers with large memory and storage capacities allows the solution of problems of increasing complexity, and a natural next step in the development of finite element procedures is the analysis of fluid flows coupled with structures.

Fluid-structure interaction analyses are increasingly required research and engineering practice, where a wide variety of applications can be found. Particularly, there is an increased interest in new and exciting areas of applications such as biomechanics, to study for example the flow of blood in arteries and veins, and the development of microelectro-mechanical devices (MEMS). Some other examples include the study and optimization of break systems, shock-absorbers, hydraulic valves, pumps, etc.

There are two main approaches that have been used to numerically solve fully coupled fluid-structure interaction problems: the simultaneous solution and the partitioned procedures. In a simultaneous solution, the coupled equations are established and then solved all together. In a partitioned procedure solution variables from one field are passed to the other and each field (fluid and structure) is solved separately

iterating between the field solutions when the coupling results in significant structural deformations. As a result, in a partitioned procedure, the fully coupled fluid-structure problem can be solved using already developed field-codes.

An important feature of fluid-structure interaction problems is that the coupling strongly depends on the mathematical models employed. The variables used for structures are displacements and, sometimes, pressures. The fluid behavior, however, can be described using pressures, velocity potentials, velocities and pressures, etc. depending on the model chosen. As a result, the coupling procedure and the effect of the coupling onto the system response can vary widely. Basically, two main types of fluid-structure interaction problems can be distinguished depending on whether the fluid is modeled using the acoustic approximation or the Navier-Stokes equations.

If the fluid can be modeled using the acoustic approximation then the load of the fluid onto the structure is only due to pressure and inertial effects (viscous effects are neglected). This approximation is very useful to analyse certain problems, such as the interaction between a structure and a contained fluid. In this case a potential formulation can be used and the degrees of freedom of the fluid (velocities and pressures) are reduced to only one per node (the potential). In addition, the coupled finite element coefficient matrix can be symmetric (ϕ -formulation [1], [2]). Hence, simultaneous solution procedures are effective for this type of fluid-structure interaction problem (see also [3]). Nevertheless, partitioned procedures have also been applied to acoustic fluid-structure interaction problems [4].

If convective terms are important the fluid is modeled using the Navier-Stokes or Euler equations. In this case usually large (non-symmetric) fluid coefficient matrices result. In addition, completely different meshes need generally be used in practice to discretize the fluid domain and the structure. Therefore, partitioned procedures are frequently preferred and used. Bathe et. al describe a general and widely employed partitioned procedure to solve fluid flow-structural interaction problems [5], [6], [7]. Stability and accuracy characteristics of partitioned procedures for some special cases have been studied in [8], [9]. Other recent works on partitioned procedures include [10], [11], [12].

Using a partitioned procedure, a relatively large number of iterations may be required at each time (or load) step to solve problems in which the structure is very compliant. If the iterations are not performed in each step, the solution accuracy frequently deteriorates rapidly. This phenomenon is like in the analysis of nonlinear structural dynamic problems where it was long ago realized that iterations are needed [2] [13].

Simultaneous solution procedures have also been used in fluid-structure interaction problems, see [14], [15], [16], [17], [18]. Since the finite element coefficient matrix of the Navier-Stokes or Euler equations is non-symmetric due to the presence of convective terms, the cost of the computations for the simultaneous solution procedure dramatically increases with the degrees of freedom considered, and therefore most research was directed to the development of partitioned procedures.

An important issue in the analysis of fluid flow-structural interaction problems is the coupling procedure employed in both the simultaneous solution and partitioned procedures.

In this thesis, we concentrate on the analysis of structures interacting with viscous fluid flows, modeled using the Navier-Stokes equations. The structure is assumed to be elastic and the fluid is assumed to be an (almost) incompressible medium. We also assume that the effect of the coupling between the fluid and the structure is significant. Hence, when using a partitioned procedure iterations between the field solutions are required. The focus of this thesis is on the coupling procedure employed in a simultaneous solution, the time integration schemes used, and how to decrease the solution time by condensation of the internal structural degrees of freedom.

The thesis is organized as follows. In the second chapter, some relevant mathematical models of fluids and structures are presented. In addition, the Lagrangian, Eulerian and arbitrary Lagrangian-Eulerian descriptions of motion are discussed. In chapter 3, usual finite element discretizations for both fluids and structures are shown. Available procedures to solve fluid flow-structural interaction problems are discussed in chapter 4 and a different approach is proposed and analyzed. A stability analysis of the proposed algorithm is presented in chapter 5. In chapter 6, the solutions of

example problems are shown to demonstrate the capabilities of the proposed scheme. Finally in chapter 7 conclusions are given.

Chapter 2

Governing equations

Governing differential equations describe the motion of continuous media. They are derived using the laws of physics (Newton's law, mass and energy conservation principles) and the constitutive relations.

Usually, structural equations of motion are written using the Lagrangian formulation, i.e. following the body particles, and the fluid flow equations are written using the Eulerian formulation, i.e. at a fixed spatial position. For fluid flow-structural interaction problems a combination of both formulations, an arbitrary Lagrangian-Eulerian formulation, is required to describe the fluid flow because the fluid domain changes as a function of time due to structural interactions.

In this chapter the Lagrangian, Eulerian and arbitrary Lagrangian-Eulerian formulations are briefly discussed. Governing and constitutive equations of Newtonian fluid flows and elastic isotropic solids are considered. Finally, the equilibrium and compatibility conditions that must be satisfied at the fluid flow-structural interface are given.

2.1 Kinematics of continuous media

Consider a body (or a part of it) that is moving through space. The space occupied by the body at time $t = 0$ is called the *reference configuration*, and the space occupied by the body at time t is called the *spatial configuration* (see figure 2-1).

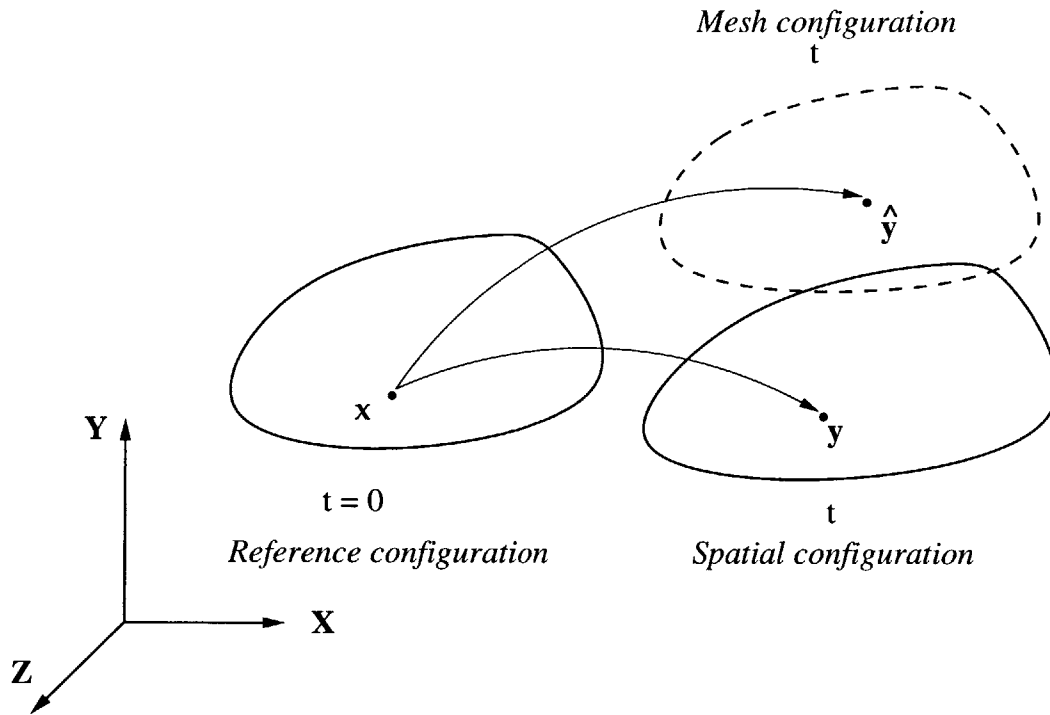


Figure 2-1: Reference, spatial and mesh configurations.

At time $t = 0$ we can identify each particle of the body with a reference coordinate \mathbf{x} . At time t the particle will be at a different position \mathbf{y} . In other words, \mathbf{y} is the position at time t of the particle that was at \mathbf{x} at time $t = 0$. Similarly, at time $t = 0$ we can identify each mesh point with a reference coordinate \mathbf{x} . At time t the mesh point will be at a different position $\hat{\mathbf{y}}$ (that is not necessarily the same as the particle positions \mathbf{y}). Then, $\hat{\mathbf{y}}$ is the position at time t of the mesh point that was at \mathbf{x} at time $t = 0$.

There are different ways of describing the motion of the body (see, for example, [19]). Three of them will be considered here,

- Lagrangian formulation
- Eulerian formulation
- Arbitrary Lagrangian-Eulerian (ALE) formulation

Equations of motion are generally written in terms of *material* or *physical particles*.

For example, when we say that a fluid is incompressible we mean that a particle cannot change its density with time, but different particles can have different densities. Newton's law of motion states that the rate of change of momentum of a body is equal to the sum of the external forces applied to that body, i.e. the law applies over a group of particles that are followed as a function of time.

In general, when solving a dynamic problem using finite element methods, any of the above descriptions can be employed (see [2], [16]). The finite element mesh can be moving with the body particles, can be fixed in space, or moving at an arbitrary velocity, and therefore we need to express the equations of motion using different formulations.

2.1.1 Lagrangian formulation

In the Lagrangian formulation, the body particles are identified in the reference configuration, at time $t = 0$, and their movement is followed as a function of time. The variables used to describe the equations of motion are then \mathbf{x} and t . This description is usually employed to describe the motion of solids, for which the reference configuration is known.

We are interested in expressing the equations of motion that are written in the Lagrangian formulation (following the particle) in the Eulerian and ALE formulations. In particular, the time derivatives that appear in the conservation laws need to be transformed.

2.1.2 Eulerian formulation

In the Eulerian formulation, the variables used in the description of the motion are \mathbf{y} and t . The movement is described at a fixed spatial position \mathbf{y} . The position occupied at $t = 0$ by the particle that is at \mathbf{y} at time t is not important and usually not known. This description is generally used to describe fluid flows.

At time t the position of a *particle* can be expressed as a function of the particle position in the reference configuration

$$\mathbf{y} = \chi(\mathbf{x}, t) \quad (2.1)$$

If equation (2.1) is known, then the velocity of a *particle* can be calculated by taking the partial derivative of (2.1) with \mathbf{x} held constant

$$\mathbf{v} = \left(\frac{\partial \mathbf{y}}{\partial t} \right)_{\mathbf{x}} \quad (2.2)$$

Also, the acceleration of the particle is

$$\mathbf{a} = \left(\frac{\partial \mathbf{v}}{\partial t} \right)_{\mathbf{x}} \quad (2.3)$$

In the Eulerian formulation, a physical quantity is known as a function of a fixed spatial position \mathbf{y} , that is to say

$$f = g(\mathbf{y}, t) = G(\chi(\mathbf{x}, t)) \quad (2.4)$$

The time derivative of the physical quantity f with \mathbf{x} held constant, is called the *material time derivative*, and is equal to the rate of change of f at the particle, i.e. as seen by an observer who is moving with the particle. The following notation is used from now on to refer to the material time derivative

$$\frac{Df}{Dt} \equiv \left(\frac{\partial f}{\partial t} \right)_{\mathbf{x}} \quad (2.5)$$

2.1.3 Arbitrary Lagrangian-Eulerian formulation

The ALE formulation is a combination of the Lagrangian and Eulerian formulations. The movement of the body is described at an arbitrary position $\hat{\mathbf{y}}$ that can change as a function of time. In a finite element analysis, the position $\hat{\mathbf{y}}$ is associated with a mesh point, and the space occupied by the mesh at time t is called the *mesh configuration* (see figure 2-1).

In the ALE formulation, the values of a physical quantity f are known as a function of a fixed mesh referential position $\hat{\mathbf{y}}$.

At time t each point $\hat{\mathbf{y}}$ can be associated to a referential position \mathbf{x} using the mapping

$$\hat{\mathbf{y}} = \hat{\chi}(\mathbf{x}, t) \quad (2.6)$$

Then, the physical quantity f can be expressed as

$$f = \hat{g}(\hat{\mathbf{y}}, t) = \hat{G}(\hat{\chi}(\mathbf{x}, t), t) \quad (2.7)$$

2.2 Lagrangian form of the conservation equations

Considerations in this work are restricted to isothermal processes, and therefore the energy conservation equation is not needed in the description of motion. In this section, the mass and momentum conservation equations in the Lagrangian formulation are given.

2.2.1 Mass conservation

The principle of mass conservation states that mass cannot be created or destroyed within a (nonrelativistic) system. This means that the amount of mass enclosed in a *material volume* (one that is fixed to the physical particles) will not change in time. The simplest form of the mass conservation principle is then

$$\frac{Dm}{Dt} = \frac{D}{Dt} \left[\int_{\Omega(t)} \rho(\mathbf{x}) \, d\Omega \right] = 0 \quad (2.8)$$

where $\Omega(t)$ is the material volume (body volume), m is the total mass enclosed in Ω and ρ is the body density.

2.2.2 Momentum conservation

Newton's law of motion can be expressed as

$$\frac{D\mathbf{P}}{Dt} = \sum \mathbf{F}_{ext} \quad (2.9)$$

where $\mathbf{P} = m\mathbf{v}$ is the momentum, $\frac{D\mathbf{P}}{Dt}$ is the instantaneous rate of change of momentum of the body at time t , and $\sum \mathbf{F}_{ext}$ is the sum of all external forces acting on the body at time t .

The equation of conservation of momentum can be written as

$$\frac{D}{Dt} \left[\int_{\Omega(t)} \rho \mathbf{v} d\Omega \right] = \sum \mathbf{F}_{ext}(t) \quad (2.10)$$

where Ω indicates the material volume.

2.3 ALE form of the conservation equations

In this section, the ALE forms of the mass and momentum conservation equations are derived using the control volume technique.

2.3.1 Mass conservation

We are interested in describing the mass conservation principle with respect to an arbitrary chosen control volume which can be moving and deforming. Using the Reynold's transport theorem [20], the mass conservation equation (2.8) can be written as

$$\frac{Dm}{Dt} = \frac{\partial}{\partial t} \int_{\hat{V}(t)} \rho d\hat{V} + \int_{\hat{S}(t)} \rho (\mathbf{v} - \hat{\mathbf{v}}) \cdot \mathbf{n} d\hat{S} = 0 \quad (2.11)$$

where $\hat{V}(t)$ is an arbitrary control volume, $\hat{S}(t)$ the control volume surface, \mathbf{v} is the fluid velocity with respect to a fixed spatial reference frame, $\hat{\mathbf{v}}$ is the velocity of the control volume, and $\partial/\partial t$ is the time derivative with \mathbf{y} held constant, or spatial time derivative.

The first term expresses the instantaneous rate of change of mass within the control volume, while the second takes into account the mass which is entering (and

leaving) the control volume through its surface at a relative velocity $\mathbf{v}_r = \mathbf{v} - \hat{\mathbf{v}}$.

Using the divergence theorem, equation (2.11) becomes

$$\frac{\partial}{\partial t} \int_{\hat{V}(t)} \rho \, d\hat{V} + \int_{\hat{V}(t)} \nabla \cdot [\rho (\mathbf{v} - \hat{\mathbf{v}})] \, d\hat{V} = 0 \quad (2.12)$$

In evaluating the first term of equation (2.12), the change of the control volume with time has to be considered.

Using Cartesian coordinates, the determinant of the Jacobian of the transformation from material coordinates to mesh referential coordinates is defined as [21]

$$\hat{J} = \det \left(\frac{\partial \hat{y}_i}{\partial x_j} \right) \quad (2.13)$$

where \hat{y}_i and x_j are the components of $\hat{\mathbf{y}}$ and \mathbf{x} , respectively.

Then,

$$d\hat{V} = \hat{J} \, dV_0 \quad (2.14)$$

where $d\hat{V}$ is a differential control volume and dV_0 is the differential control volume in the initial configuration, $dV_0 = d\hat{V}(t = 0)$.

The spatial time derivative of \hat{J} is

$$\frac{\partial \hat{J}}{\partial t} = \hat{J} \nabla \cdot \hat{\mathbf{v}} \quad (2.15)$$

and therefore

$$\frac{\partial}{\partial t} \int_{\hat{V}(t)} \rho \, d\hat{V} = \frac{\partial}{\partial t} \int_{V(0)} \rho \, \hat{J} \, dV_0 = \int_{\hat{V}(t)} \left(\frac{\partial \rho}{\partial t} \right)_{\hat{\mathbf{y}}} \, d\hat{V} + \int_{\hat{V}(t)} \rho \nabla \cdot \hat{\mathbf{v}} \, d\hat{V} \quad (2.16)$$

Substituting (2.16) into (2.12) we obtain

$$\rho^* + (\mathbf{v} - \hat{\mathbf{v}}) \nabla \rho + \rho \nabla \cdot \mathbf{v} = 0 \quad (2.17)$$

where the superscript * indicates time derivative with respect to a fixed mesh point,

i.e. is the rate of change as seen by an observer that is moving with the mesh point.

Expression (2.17) is the differential equation of mass conservation written in the ALE formulation of motion.

The *material* rate of change of the density $\frac{D\rho}{Dt}$ can then be written as

$$\frac{D\rho}{Dt} = \rho^* + (\mathbf{v} - \hat{\mathbf{v}}) \cdot \nabla \rho \quad (2.18)$$

and expresses the density changes of the *material* or *physical particles* as a function of time.

Note that if $\hat{\mathbf{v}} = 0$ or $\hat{\mathbf{v}} = \mathbf{v}$ in equation (2.17) the Eulerian and Lagrangian forms of the mass conservation equation are recovered respectively.

2.3.2 Momentum conservation

We are interested in describing Newton's law of motion with respect to an arbitrary chosen control volume which can be moving and deforming. Using the Reynold's transport theorem equation (2.10) can be rewritten as

$$\frac{D}{Dt} \int_{\Omega(t)} \rho \mathbf{v} d\Omega = \frac{\partial}{\partial t} \int_{\hat{V}(t)} \rho \mathbf{v} d\hat{V} + \int_{\hat{S}(t)} \rho \mathbf{v} (\mathbf{v} - \hat{\mathbf{v}}) \cdot \mathbf{n} d\hat{S} = \sum \mathbf{F}_{ext}(t) \quad (2.19)$$

Therefore the rate of change of momentum of the body which at time t occupies the volume $\Omega \equiv \hat{V}(t)$ is equal to the rate of change of momentum of the material instantaneously inside the control volume \hat{V} at time t , plus the inward flux of momentum through the control surface [19].

The right hand side of equation (2.19) is the sum of the forces that are acting over the particles located inside Ω at time t . It is independent of the choice of description of motion. However, the expression for the material time derivative (left hand side) does depend on the description of motion.

Expression (2.19) constitutes a system of three equations (one for each component of the vector \mathbf{v}). Expressing \mathbf{v} in a Cartesian coordinate system, where the v_i are the

components of \mathbf{v} , and using the divergence theorem

$$\frac{\partial}{\partial t} \int_{\hat{V}(t)} \rho v_i d\hat{V} + \int_{\hat{V}(t)} \nabla \cdot [\rho v_i (\mathbf{v} - \hat{\mathbf{v}})] d\hat{V} = \sum \mathbf{F}_{ext,i}(t) \quad (2.20)$$

Using equations (2.14) and (2.15)

$$\frac{\partial}{\partial t} \int_{\hat{V}(t)} \rho v_i d\hat{V} = \int_{\hat{V}(t)} (\rho v_i)^* d\hat{V} + \int_{\hat{V}(t)} \rho v_i \nabla \cdot \hat{\mathbf{v}} d\hat{V} \quad (2.21)$$

Substituting equation (2.21) into equation (2.20) and after some algebra,

$$v_i [\rho^* + (\mathbf{v} - \hat{\mathbf{v}}) \cdot \nabla \rho + \rho \nabla \cdot \mathbf{v}] + \rho [v_i^* + (\mathbf{v} - \hat{\mathbf{v}}) \cdot \nabla v_i] = f_{ext,i} \quad (2.22)$$

where $f_{ext,i}$ are the components of external forces per unit volume (in Cartesian coordinates).

The first term in square brackets in equation (2.22) is the mass conservation equation (2.17), and therefore cancels out. Then, the momentum conservation equation in the ALE formulation can be written as

$$\rho \{ \mathbf{v}^* + [(\mathbf{v} - \hat{\mathbf{v}}) \cdot \nabla] \mathbf{v} \} = \mathbf{f}_{ext} \quad (2.23)$$

and the material rate of change of momentum is

$$\rho \frac{D\mathbf{v}}{Dt} = \rho \{ \mathbf{v}^* + [(\mathbf{v} - \hat{\mathbf{v}}) \cdot \nabla] \mathbf{v} \} \quad (2.24)$$

The Eulerian and Lagrangian descriptions of motion can be recovered by assuming $\hat{\mathbf{v}} = 0$ and $\hat{\mathbf{v}} = \mathbf{v}$ in equation (2.23) respectively.

2.4 Fluid flow equations

The fluid flow equations of motion are derived from the momentum and mass conservation equations, (2.23) and (2.17), and appropriate constitutive laws. In what follows, some relevant fluid models are described. Since in a fluid flow-structural interaction problem, in general, the fluid domain changes as a function of time (due to

the interaction with the structure), the equations of motion of the fluid are expressed using the ALE formulation.

2.4.1 Compressible fluid

Using the ALE formulation, the Navier-Stokes equations are

$$\rho \{ \mathbf{v}^* + [(\mathbf{v} - \hat{\mathbf{v}}) \cdot \nabla] \mathbf{v} \} = \nabla \cdot \boldsymbol{\tau}^F + \mathbf{f}^B \quad (2.25)$$

$$\rho^* + (\mathbf{v} - \hat{\mathbf{v}}) \cdot \nabla \rho + \rho \nabla \cdot \mathbf{v} = 0 \quad (2.26)$$

where equation (2.25) is the momentum conservation and equation (2.26) is continuity equation.

The constitutive relations for a Newtonian fluid (in Cartesian coordinates) are

$$\tau_{ij}^F = (-p + \lambda e_{kk}) \delta_{ij} + 2\mu e_{ij} \quad (2.27)$$

with

$$e_{ij} = \frac{1}{2} (v_{i,j} + v_{j,i}) \quad (2.28)$$

In these relations, $\boldsymbol{\tau}^F$ is the stress tensor in the fluid, \mathbf{f}^B is the vector of body forces, p is the pressure, ρ is the fluid density, μ is the dynamic viscosity coefficient, λ is the second coefficient of viscosity and e_{ij} is the (i,j) th component of the velocity strain tensor.

For an isotropic Newtonian compressible fluid, the Stokes' hypothesis, $\lambda = -\frac{2}{3}\mu$, is usually a good approximation, and the constitutive equations for a compressible fluid become,

$$\tau_{ij}^F = -p \delta_{ij} + 2\mu \left(e_{ij} - \frac{e_{kk}}{3} \delta_{ij} \right) \quad (2.29)$$

The boundary conditions required to solve (2.25) and (2.26) can be given as fol-

lows:

$$\mathbf{v} = \mathbf{v}^s \quad \text{in } S_v^F \quad (2.30)$$

$$\boldsymbol{\tau}^F \mathbf{n}^F = \mathbf{t}_f^s \quad \text{in } S_f^F \quad (2.31)$$

and initial condition

$$\mathbf{v}(t = 0) = \mathbf{v}_0 \quad (2.32)$$

where S_v^F is the part of the boundary with imposed velocities \mathbf{v}^s , S_f^F is the part of the boundary with imposed surface forces \mathbf{t}_f^s and \mathbf{n}^F is the unit outward vector normal to the fluid boundary.

2.4.2 Incompressible fluid

For the case of an incompressible fluid, the density of a particle does not change as a function of time ($D\rho/Dt = 0$) and the continuity equation for a fully incompressible fluid reduces to

$$\nabla \cdot \mathbf{v} = 0 \quad (2.33)$$

2.4.3 Almost incompressible flow

For an almost incompressible fluid, the density can be expressed as $\rho = \rho_o + \Delta\rho$, and $\Delta\rho/\rho_o \ll 1$, such that $\rho \approx \rho_o$ can be assumed.

The bulk modulus of a fluid or solid, κ , is defined as

$$\kappa = \rho_o \left(\frac{\partial p}{\partial \rho} \right)_T \quad (2.34)$$

and therefore is a measure of the change of density due to a change of pressure at constant temperature T . Then,

$$\frac{1}{\rho_o} \frac{D\rho}{Dt} = \frac{1}{\rho_o} \left(\frac{\partial \rho}{\partial p} \right)_T \frac{Dp}{Dt} = \frac{1}{\kappa} \frac{Dp}{Dt} \quad (2.35)$$

Using equation (2.35) the continuity equation for an almost incompressible fluid becomes

$$\frac{1}{\kappa} [p^* + (\mathbf{v} - \hat{\mathbf{v}}) \cdot \nabla p] + \nabla \cdot \mathbf{v} = 0 \quad (2.36)$$

and the e_{kk} term in the constitutive equation (2.29) is neglected.

2.5 Structural equations

In general, structural equations are written using the Lagrangian formulation. The equations of motion are derived from the momentum equations using appropriate constitutive relations. In what follows, the equations of an isotropic elastic material will be described.

2.5.1 Isotropic linear elastic material

Neglecting damping effects, the momentum equations for a structure are

$$\rho \frac{D\mathbf{v}}{Dt} = \rho \frac{D^2\mathbf{u}}{Dt^2} = \nabla \cdot \boldsymbol{\tau}^S + \mathbf{f}^B \quad (2.37)$$

The constitutive relations for a linear elastic isotropic material (in Cartesian coordinates) are

$$\tau_{ij}^S = \frac{E\nu}{(1+\nu)(1-2\nu)} \varepsilon_{kk} \delta_{ij} + \frac{E}{1+\nu} \varepsilon_{ij} \quad (2.38)$$

with

$$\varepsilon_{ij} = \frac{1}{2} (u_{i,j} + u_{j,i}) \quad (2.39)$$

Here \mathbf{u} is the vector of structural displacements, $\boldsymbol{\tau}^S$ is the stress tensor, \mathbf{f}^B is the

vector of body forces, ρ is the density of the structure, E is the elastic or Young's modulus, ν is Poisson's ratio, and the ε_{ij} is the (ij) th component of the strain tensor.

The boundary conditions needed to solve equation (2.37) are

$$\mathbf{u} = \mathbf{u}^s \quad \text{in } S_u^S \quad (2.40)$$

$$\boldsymbol{\tau}^S \mathbf{n}^S = \mathbf{t}_s^s \quad \text{in } S_f^S \quad (2.41)$$

and initial conditions

$$\mathbf{u}(t = 0) = \mathbf{u}_0; \quad \dot{\mathbf{u}}(t = 0) = \dot{\mathbf{u}}_0 \quad (2.42)$$

where S_u^S is the part of the structural boundary with imposed displacements \mathbf{u}^s , S_f^S is the part of the boundary with imposed surface forces \mathbf{t}_s^s and \mathbf{n}^S is the unit outward vector normal to the structural boundary.

Since the equations of motion of the solid are described using the Lagrangian formulation, no convective terms are present. Furthermore, because in the Lagrangian formulation the particles are being followed, the mass conservation is automatically satisfied and there is no need to impose it separately as was the case for the fluid flow equations.

For an almost incompressible material ($\nu \rightarrow 0.5$) numerical problems can be expected when using the constitutive relations (2.38). To overcome this problem (see [2]), the pressure is introduced in the finite element equations as a separate degree of freedom and mixed interpolated elements are used.

The pressure is equal to

$$p = -\frac{\tau_{\alpha\alpha}^S}{3} = -\kappa \varepsilon_{\alpha\alpha} \quad (2.43)$$

Introducing the pressure into the constitutive relations (2.38),

$$\tau_{ij}^S = -p \delta_{ij} + \frac{E}{(1 + \nu)} \varepsilon'_{ij} \quad (2.44)$$

where ε'_{ij} are the deviatoric strain components

$$\varepsilon'_{ij} = \varepsilon_{ij} - \frac{\varepsilon_{\alpha\alpha}}{3} \delta_{ij} \quad (2.45)$$

Another equation is needed to relate the pressure to the displacements. This relation is provided by (2.43) and the relation between the bulk modulus of the material and the Young's modulus and Poisson's ratio

$$\kappa = \frac{E}{3(1 - 2\nu)} \quad (2.46)$$

2.6 Fluid flow-structural interface conditions

We are interested in coupled systems where fluid flow-structural interactions take place. Hence, in addition to the fluid and structural equations, equilibrium and compatibility conditions must be satisfied at the fluid-structure interface.

The equilibrium conditions at the interface can be expressed as

$$\boldsymbol{\tau}^F \mathbf{n}^F + \boldsymbol{\tau}^S \mathbf{n}^S = 0 \quad (\text{at interface}) \quad (2.47)$$

where \mathbf{n}^F and \mathbf{n}^S are unit normal surface vectors pointing outward of the fluid and structural domains respectively.

This condition ensures that the forces are in equilibrium at the fluid-structure interface.

The compatibility condition at the interface requires that

$$\hat{\mathbf{u}}_f^I = \mathbf{u}_s^I \quad (\text{at interface}) \quad (2.48)$$

where $\hat{\mathbf{u}}_f^I$ is the vector of displacements of the fluid (domain) at the interface and \mathbf{u}_s^I is the vector of displacements of the structure at the interface.

This condition ensures that the material will not overlap and no gaps will be formed at the interface.

Chapter 3

Finite element formulation

In a finite element formulation, the weak (or variational) forms of the governing differential equations of motion are considered, and using the Galerkin procedure the test functions correspond to the finite element interpolations.

In what follows, some spaces needed in the formulation of the finite element method will be defined (see also [2], [22]).

Let us denote by Ω a bounded domain in \mathfrak{R}^n (with $n = 2$ or 3) and by S its boundary.

$L^2(\Omega)$ represents the space of functions that are square integrable over Ω ,

$$L^2(\Omega) = \{q : \int_{\Omega} q^2 d\Omega < +\infty\}$$

Similarly, $\mathbf{L}^2(\Omega)$ is the space of vector functions that are square integrable over Ω ,

$$\mathbf{L}^2(\Omega) = \{\mathbf{q} : \int_{\Omega} \sum_i q_i^2 d\Omega < +\infty\}$$

The Sobolev space is defined for any non-negative integer value k as the space of square integrable functions over Ω , whose derivatives up to order k are also square integrable over Ω

$$H^k(\Omega) = \{q \in L^2(\Omega) : \partial^n q \in L^2(\Omega) \quad \forall |n| \leq k\}$$

For vector valued functions, we have

$$\mathbf{H}^k(\Omega) = \{\mathbf{v} : v_i \in H^k(\Omega)\}$$

3.1 Fluid flow discretization

The variational formulation of an almost incompressible fluid modeled using the Navier-Stokes equations and expressed in the ALE description of motion (in Cartesian coordinates) can be stated as:

Given \mathbf{f}^B , find $\mathbf{v} \in \mathbf{H}^1(\hat{V})$ with $\mathbf{v}|_{S_v} = \mathbf{v}^s$ and $p \in H^1(\hat{V})$ such that

$$\int_{\hat{V}} \bar{v}_i \rho [v_i^* + v_{i,j} (v_j - \hat{v}_j)] d\hat{V} + \int_{\hat{V}} \bar{e}_{ij} \tau_{ij}^F d\hat{V} = \mathfrak{R}^F \quad (3.1)$$

$$\int_{\hat{V}} \frac{\bar{p}}{\kappa} [p^* + p_{,i} (v_i - \hat{v}_i)] d\hat{V} + \int_{\hat{V}} \bar{p} v_{i,i} d\hat{V} = 0 \quad (3.2)$$

with

$$\mathfrak{R}^F = \int_{\hat{V}} \bar{v}_i f_i^B d\hat{V} + \int_{S_f} \bar{v}_i^{S_f} f_i^{S_f} dS + \int_{S_I} \bar{v}_i^{S_I} f_i^{S_S} dS \quad (3.3)$$

where $\bar{\mathbf{v}} \in \mathbf{H}^1(\hat{V})$ and $\bar{p} \in H^1(\hat{V})$ are the virtual velocity and pressure, \hat{V} is the volume of the fluid domain, \mathbf{v} and p are the velocity and pressure functions to be calculated, $\hat{\mathbf{v}}$ is the mesh velocity, \bar{e}_{ij} and τ_{ij}^F are the (i,j) th components of the virtual velocity strain tensor and the stress tensor respectively, κ is the bulk modulus, S_v is the part of the boundary with prescribed velocity \mathbf{v}^s , S_f is the part of the fluid boundary with prescribed tractions of components $f_i^{S_f}$, and S_I is the part of the boundary corresponding to the interface, where tractions with components $f_i^{S_S}$ are exerted by the structure onto the fluid.

If the fluid is incompressible, $\kappa \rightarrow \infty$, and the term containing κ in equation (3.2) vanishes.

Equations (3.1) and (3.2) must be discretized in space in order to be solved numerically. The following finite element spaces are introduced for the velocity and

pressure,

$$V^h = \{\mathbf{v}^h \in \mathbf{H}^1(\hat{V}), \mathbf{v}^h|_{S_v} = \mathbf{v}^s(t)\} \quad (3.4)$$

$$\bar{V}^h = \{\bar{\mathbf{v}}^h \in \mathbf{H}^1(\hat{V}), \mathbf{v}^h|_{S_v} = 0\} \quad (3.5)$$

$$Q^h = \{p^h \in H^1(\hat{V})\} \quad (3.6)$$

$$\bar{Q}^h = \{\bar{p}^h \in H^1(\hat{V})\} \quad (3.7)$$

Therefore, the finite element problem can be stated as:

Given \mathbf{f}_B , find $\mathbf{v}^h \in V^h(\hat{V})$ and $p^h \in Q^h(\hat{V})$ such that

$$\int_{\hat{V}} \bar{v}_i^h \rho [(v_i^h)^* + v_{i,j}^h (v_j^h - \hat{v}_j^h)] d\hat{V} + \int_{\hat{V}} \bar{e}_{ij}^h \tau_{ij}^h{}^F d\hat{V} = \mathfrak{R}^F \quad (3.8)$$

$$\int_{\hat{V}} \frac{\bar{p}^h}{\kappa} [(p^h)^* + p_{,i}^h (v_i^h - \hat{v}_i^h)] d\hat{V} + \int_{\hat{V}} \bar{p}^h v_{i,i}^h d\hat{V} = 0 \quad (3.9)$$

with

$$\mathfrak{R}^F = \int_{\hat{V}} \bar{v}_i^h f_i^B d\hat{V} + \int_{S_f} (\bar{v}_i^h)^{S_f} f_i^{S_f} dS + \int_{S_I} (\bar{v}_i^h)^{S_I} f_i^{S_S} dS \quad (3.10)$$

for all $\bar{\mathbf{v}}^h \in \bar{V}^h(\hat{V})$ and $\bar{p}^h \in \bar{Q}^h(\hat{V})$.

In the finite element procedure, the space V^h depends on the elements chosen to discretize the volume \hat{V} . In a 2D space, we can choose, for example, quadrilateral bilinear or parabolic elements. The pressure interpolation, however, cannot be chosen arbitrarily (see for example [2], [22]), otherwise, the formulation may not be stable. In order to have a stable scheme, the *inf-sup* condition must be satisfied. In this thesis, 9/3 elements, which satisfy the inf-sup condition, are used to calculate the fluid response of the coupled system. The 9/3 element is a quadrilateral 9 node element, in which the velocities are interpolated from the 9 nodes and the pressure

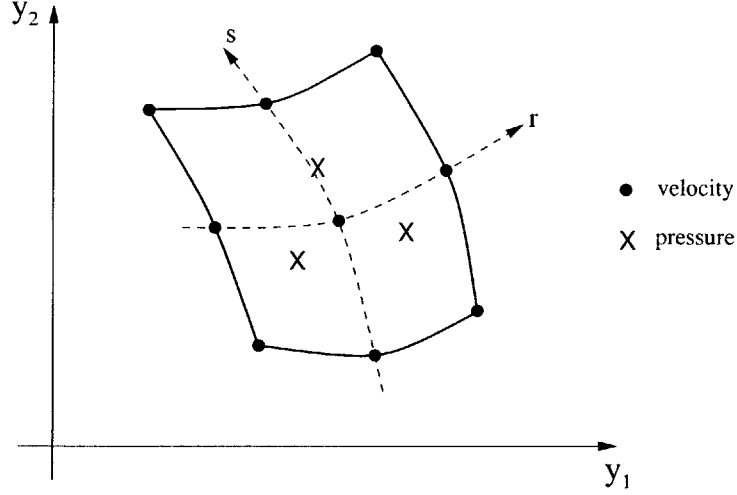


Figure 3-1: 9/3 element.

is taken to be a linear function inside the element (3 unknowns per element) and discontinuous across elements, see figure (3-1).

The solution obtained using the discretized equations (3.8) and (3.9) is good for low Reynolds (Re) number flows. However, if the Reynolds number is increased, oscillations appear due to the presence of the convective terms $(\mathbf{v} - \hat{\mathbf{v}}) \cdot \nabla \mathbf{v}$ (here the Re number is based on the relative velocity $\mathbf{v}_r = \mathbf{v} - \hat{\mathbf{v}}$). To avoid oscillations, *upwinding* is introduced into the equations. The idea is to introduce some artificial diffusivity to stabilize the convective term but without degrading the accuracy of the solution (see for example [23], [2], [24]). In this work, the following upwind terms, proposed by D. Hendriana and K.J. Bathe [25], are used

$$\sum_m \int_{\hat{V}^{(m)}} \frac{\partial^2 \bar{v}_i}{\partial y_j^2} \tau_j |v_j - \hat{v}_j| \frac{\partial^2 v_i}{\partial y_j^2} d\hat{V}^{(m)} \quad (3.11)$$

and

$$\tau_j = \frac{1}{9} \left[\left(\frac{\partial y_j}{\partial r} \right)^2 + \left(\frac{\partial y_j}{\partial s} \right)^2 \right]^{3/2} \quad (3.12)$$

where $\hat{V}^{(m)}$ is the m^{th} element volume (2D), the y_i are the coordinates of the body

in a fixed Cartesian coordinate system, and r, s are the isoparametric coordinates of the element (see figure 3-1).

Note that a convective term is also present in the continuity equation, however, the velocity is divided by κ , which is usually a very large constant ($\sim 10^9$ Pa for water, for example), and therefore, an upwind term will not be necessary in the continuity equation.

The dynamic equations of the fluid flow, including the upwinding can be represented as

$${}^{t+\Delta t}W = {}^{t+\Delta t}W_{NS} + {}^{t+\Delta t}W_{UP} = {}^{t+\Delta t}R \quad (3.13)$$

where ${}^{t+\Delta t}W_{NS}$ and ${}^{t+\Delta t}W_{UP}$ represent the terms coming from the standard Galerkin procedure and the upwind terms respectively, and ${}^{t+\Delta t}R$ is the known load vector due to boundary conditions.

Because equations (3.13) are nonlinear, to obtain an accurate solution at time $t + \Delta t$ the equations are linearized and iterations are performed at each time step using, for example, the Newton-Raphson procedure.

Using a Taylor series expansion of (3.13) in time

$${}^{t+\Delta t}W \simeq {}^tW + {}^tW^* \Delta t \quad (3.14)$$

and equation (3.13) can be expressed as

$${}^tW^* \Delta t \simeq {}^{t+\Delta t}R - {}^tW \quad (3.15)$$

To calculate the time derivative ${}^tW^* = \left(\frac{\partial W}{\partial t}\right)_{\hat{y}}$, we have to consider that the volume \hat{V} is moving and deforming.

In deriving the expressions for ${}^tW^*$, the following identities are useful (see for example [21], [26], [27] and chapter 2)

$$\frac{\partial}{\partial t} \int_{\hat{V}} g \, d\hat{V} = \frac{\partial}{\partial t} \int_{\hat{V}_0} g \, \hat{J} \, d\hat{V}_0 = \int_{\hat{V}} [g^* + g \nabla \cdot \hat{\mathbf{v}}] \, d\hat{V} \quad (3.16)$$

$$\left(\frac{\partial a}{\partial y_i}\right)^* = \frac{\partial a^*}{\partial y_i} - \frac{\partial a}{\partial y_k} \frac{\partial \hat{v}_k}{\partial y_i} \quad (3.17)$$

Equation (3.16) is derived from equation (2.14) and (2.15). Equation (3.17) can be derived as follows

$$\begin{aligned} \left(\frac{\partial a}{\partial y_i}\right)^* &= \frac{\partial}{\partial t} \left(\frac{\partial a}{\partial y_i}\right) + \frac{\partial}{\partial y_k} \left(\frac{\partial a}{\partial y_i}\right) \hat{v}_k \\ &= \frac{\partial}{\partial y_i} \left(\frac{\partial a}{\partial t}\right) + \frac{\partial}{\partial y_i} \left(\frac{\partial a}{\partial y_k} \hat{v}_k\right) - \frac{\partial a}{\partial y_k} \frac{\partial \hat{v}_k}{\partial y_i} \\ &= \frac{\partial a^*}{\partial y_i} - \frac{\partial a}{\partial y_k} \frac{\partial \hat{v}_k}{\partial y_i} \end{aligned} \quad (3.18)$$

Hence, the expressions for ${}^tW^*$ become (see also [26], [27])

$$\begin{aligned} {}^tW_{NS(v)}^* \Delta t &= \int_{\hat{V}} \rho \bar{v}_i \left[\Delta v_i^* + (\Delta v_k - \Delta \hat{v}_k) \frac{\partial v_i}{\partial y_k} + (v_k - \hat{v}_k) \left(\frac{\partial \Delta v_i}{\partial y_k} - \frac{\partial v_i}{\partial y_j} \frac{\partial \Delta \hat{u}_j}{\partial y_k} \right) \right] d\hat{V} - \\ &\quad - \int_{\hat{V}} \left(\Delta p \frac{\partial \bar{v}_k}{\partial y_k} - p \frac{\partial \bar{v}_k}{\partial y_j} \frac{\partial \Delta \hat{u}_j}{\partial y_k} + p \frac{\partial \bar{v}_j}{\partial y_j} \frac{\partial \Delta \hat{u}_k}{\partial y_k} - \mu \frac{\partial \bar{v}_k}{\partial y_n} \frac{\partial \Delta v_k}{\partial y_n} \right) d\hat{V} - \\ &\quad - \int_{\hat{V}} \mu \left(\frac{\partial \bar{v}_k}{\partial y_i} \frac{\partial \Delta \hat{u}_i}{\partial y_n} \frac{\partial v_k}{\partial y_n} + \frac{\partial \bar{v}_k}{\partial y_n} \frac{\partial v_k}{\partial y_i} \frac{\partial \Delta \hat{u}_i}{\partial y_n} - \frac{\partial \bar{v}_k}{\partial y_n} \frac{\partial v_k}{\partial y_n} \frac{\partial \Delta \hat{u}_i}{\partial y_i} \right) d\hat{V} + \\ &\quad + \int_{\hat{V}} \bar{v}_i \left\{ \rho \left[v_i^* + (v_k - \hat{v}_k) \frac{\partial v_i}{\partial y_k} \right] - f_i^F \right\} \frac{\partial \Delta \hat{u}_n}{\partial y_n} d\hat{V} \end{aligned} \quad (3.19)$$

$$\begin{aligned} {}^tW_{NS(p)}^* \Delta t &= - \int_{\hat{V}} \bar{p} \left\{ \frac{\partial \Delta v_k}{\partial y_k} - \frac{\partial v_k}{\partial y_n} \frac{\partial \Delta \hat{u}_n}{\partial y_k} + \frac{1}{\kappa} \left[\Delta p^* + (\Delta v_k - \Delta \hat{v}_k) \frac{\partial p}{\partial y_k} \right] \right\} d\hat{V} + \\ &\quad + \int_{\hat{V}} \frac{\bar{p}}{\kappa} \left\{ (v_k - \hat{v}_k) \frac{\partial p}{\partial y_n} \frac{\partial \Delta \hat{u}_n}{\partial y_k} - (v_k - \hat{v}_k) \frac{\partial \Delta p}{\partial y_k} \right\} d\hat{V} - \\ &\quad - \int_{\hat{V}} \bar{p} \left\{ \frac{\partial v_k}{\partial y_k} + \frac{1}{\kappa} \left[p^* + (v_k - \hat{v}_k) \frac{\partial p}{\partial y_k} \right] \right\} \frac{\partial \Delta \hat{u}_n}{\partial y_n} d\hat{V} \end{aligned} \quad (3.20)$$

$$\begin{aligned}
{}^tW_{UP}^* \Delta t &= \int_{\hat{V}} \left(-\frac{\partial \bar{v}_i}{\partial y_k} \frac{\partial^2 \Delta \hat{u}_k}{\partial y_j^2} \tau_j |v_j - \hat{v}_j| \frac{\partial^2 v_i}{\partial y_j^2} + \frac{\partial^2 \bar{v}_i}{\partial y_j^2} \Delta \tau_j |v_j - \hat{v}_j| \frac{\partial^2 v_i}{\partial y_j^2} \right) d\hat{V} + \\
&+ \int_{\hat{V}} \frac{\partial^2 \bar{v}_i}{\partial y_j^2} \tau_j |v_j - \hat{v}_j| (\Delta v_j - \Delta \hat{v}_j) \frac{\partial^2 v_i}{\partial y_j^2} d\hat{V} + \\
&+ \int_{\hat{V}} \frac{\partial^2 \bar{v}_i}{\partial y_j^2} \tau_j |v_j - \hat{v}_j| \left(\frac{\partial^2 \Delta v_i}{\partial y_j^2} - \frac{\partial v_i}{\partial y_k} \frac{\partial^2 \Delta \hat{u}_k}{\partial y_j^2} \right) d\hat{V} + \\
&+ \int_{\hat{V}} \left(\frac{\partial^2 \bar{v}_i}{\partial y_j^2} \tau_j |v_j - \hat{v}_j| \frac{\partial^2 v_i}{\partial y_j^2} \frac{\partial \Delta \hat{u}_m}{\partial y_m} \right) d\hat{V} \tag{3.21}
\end{aligned}$$

and

$$\Delta \tau_j = \frac{1}{3} \left(\frac{\partial y_j}{\partial r} + \frac{\partial y_j}{\partial s} \right) \Delta \hat{u}_j \tag{3.22}$$

where ${}^tW_{NS(v)}^*$ and ${}^tW_{NS(p)}^*$ are the contributions to ${}^tW^*$ from the momentum and continuity equations respectively, ${}^tW_{UP}^*$ is the contribution from the upwind term, and Δv_i , Δp are the increments of v_i and p . There is no sum in j in equation (3.22).

The resulting linearized finite element equations can be expressed in matrix form as

$$\begin{pmatrix} \mathbf{M}_{vv} & \mathbf{0} & \hat{\mathbf{M}}_v \\ \mathbf{0} & \mathbf{M}_{pp} & \hat{\mathbf{M}}_p \end{pmatrix} \begin{pmatrix} \dot{\mathbf{v}} \\ \dot{\mathbf{p}} \\ \dot{\hat{\mathbf{v}}} \end{pmatrix} + \begin{pmatrix} \mathbf{K}_{vv} & \mathbf{K}_{vp} & \hat{\mathbf{K}}_v \\ \mathbf{K}_{pv} & \mathbf{K}_{pp} & \hat{\mathbf{K}}_p \end{pmatrix} \begin{pmatrix} \mathbf{v} \\ \mathbf{p} \\ \hat{\mathbf{u}} \end{pmatrix} = \begin{pmatrix} \mathbf{R}_v \\ \mathbf{0} \end{pmatrix} - \begin{pmatrix} \mathbf{F}_v \\ \mathbf{F}_p \end{pmatrix} \tag{3.23}$$

where the individual matrices are obtained from the expressions of ${}^tW_{NS(v)}^*$, ${}^tW_{NS(p)}^*$ and ${}^tW_{UP}^*$; \mathbf{v} , \mathbf{p} , $\hat{\mathbf{u}}$, $\hat{\mathbf{v}}$, are the increments of velocity, pressure, mesh displacement and mesh velocity with respect to the last iteration; and \mathbf{F}_v , \mathbf{F}_p contain the known terms of the linearization. Because the mesh displacements and velocities are arbitrary, an algorithm must be provided to calculate them from the displacements and velocities at the fluid-structure interface and any other moving boundary.

3.2 Structural equations

The weak form of the transient structural equations can be stated as ([2])

Given \mathbf{f}^B , find $\mathbf{u} \in \mathbf{H}^1(\Omega)$ with $\mathbf{u}|_{S_u} = \mathbf{u}^s$ such that

$$\int_{\Omega} \bar{u}_i \rho \ddot{u}_i d\Omega + \int_{\Omega} \bar{\varepsilon}_{ij} \tau_{ij}^S d\Omega = \mathfrak{R}^S \quad (3.24)$$

with

$$\mathfrak{R}^S = \int_{\Omega} \bar{u}_i f_i^B d\Omega + \int_{S_f} \bar{u}_i^{S_f} f_i^{S_f} dS + \int_{S_I} \bar{u}_i^{S_I} f_i^{S_F} dS \quad (3.25)$$

for all $\bar{\mathbf{u}} \in \mathbf{H}^1(\Omega)$. Here Ω is the material volume, $\bar{\mathbf{u}}$ is the vector of virtual displacements, $\bar{\varepsilon}_{ij}$ and τ_{ij}^S are the (i,j) th components of the virtual strain tensor and the stress tensor respectively, \mathbf{f}^B is the vector of body forces, S_f is the part of the structural boundary with prescribed tractions of components $f_i^{S_f}$ and S_I is the part of the boundary corresponding to the fluid flow-structural interface, where tractions of components $f_i^{S_F}$ are exerted by the fluid onto the structure.

Finite element spaces for the structural equations are defined as follows,

$$V^h = \{\mathbf{u}^h \in \mathbf{H}^1(\Omega), \mathbf{u}^h|_{S_u} = \mathbf{u}^s(t)\} \quad (3.26)$$

$$\bar{V}^h = \{\bar{\mathbf{u}}^h \in \mathbf{H}^1(\Omega), \bar{\mathbf{u}}^h|_{S_u} = 0\} \quad (3.27)$$

and the spaces Q^h and \bar{Q}^h are defined by (3.6) and (3.7), respectively.

The finite element problem can be stated as

Given \mathbf{f}_B , find $\mathbf{u}^h \in V^h(\Omega)$ such that

$$\int_{\Omega} \bar{u}_i^h \rho \ddot{u}_i^h d\Omega + \int_{\Omega} \bar{\varepsilon}_{ij}^h \tau_{ij}^{hS} d\Omega = \mathfrak{R}^S \quad (3.28)$$

with

$$\mathfrak{R}^S = \int_{\Omega} \bar{u}_i^h f_i^B d\Omega + \int_{S_f} (\bar{u}_i^h)^{S_f} f_i^{S_f} dS + \int_{S_I} (\bar{u}_i^h)^{S_I} f_i^{S_F} dS \quad (3.29)$$

for all $\bar{\mathbf{u}}^h \in \bar{V}^h(\Omega)$.

Equation (3.28) is the displacement based finite element formulation for structures.

The finite element matrix equations from (3.28), neglecting damping effects, can be written as

$$\mathbf{M}_u \ddot{\mathbf{u}} + \mathbf{K}_u \mathbf{u} = \mathbf{R}_u \quad (3.30)$$

where \mathbf{M}_u and \mathbf{K}_u are the mass and stiffness matrices, and \mathbf{u} , $\ddot{\mathbf{u}}$ are the vectors of displacements and accelerations. Equation (3.30) is assumed to be linear in this thesis.

When the solid is almost incompressible, the displacement based finite element formulation fails to give accurate results (except in the two-dimensional plane stress case). To overcome this problem, mixed elements are used and the equations are re-formulated in terms of displacements and pressures. The finite element displacement/pressure formulation can then be stated as:

Given \mathbf{f}^B , find $\mathbf{u}^h \in V^h(\Omega)$ and $p^h \in Q^h(\Omega)$ such that

$$\int_{\Omega} \bar{u}_i^h \rho \ddot{u}_i^h d\Omega + \int_{\Omega} (\varepsilon_{ij}^h)' (\tau_{ij}^h)' d\Omega - \int_{\Omega} \bar{u}_{i,i}^h p^h d\Omega = \mathfrak{R}^S \quad (3.31)$$

$$- \int_{\Omega} \left(\frac{p^h}{\kappa} + u_{i,i}^h \right) \bar{p}^h d\Omega = 0 \quad (3.32)$$

for all $\bar{\mathbf{u}}^h \in \bar{V}^h$, $\bar{p}^h \in \bar{Q}^h$. Here $\boldsymbol{\varepsilon}'$ and $\boldsymbol{\tau}'$ are the deviatoric parts of the strain and stress tensors, p is the pressure and the overbar indicates virtual quantities.

The finite element matrix equations corresponding to equations (3.31) and (3.32) can be written as

$$\begin{pmatrix} \mathbf{M}_{uu} & \mathbf{0} \\ \mathbf{0} & \mathbf{0} \end{pmatrix} \begin{pmatrix} \ddot{\mathbf{u}} \\ \ddot{\mathbf{p}} \end{pmatrix} + \begin{pmatrix} \mathbf{K}_{uu} & \mathbf{K}_{up} \\ \mathbf{K}_{up}^T & \mathbf{0} \end{pmatrix} \begin{pmatrix} \mathbf{u} \\ \mathbf{p} \end{pmatrix} = \begin{pmatrix} \mathbf{R}_u \\ \mathbf{0} \end{pmatrix} \quad (3.33)$$

The elements to be used with the displacement/pressure formulation must satisfy the *inf-sup* condition in order for the system of equations to be stable. In this thesis, 9/3 mixed elements will be used when using plane-strain and axisymmetric 2D mod-

els and 9 node elements when using plane stress 2D models (and the displacement formulation). Displacement based formulations can be used with 2D plane stress models even if the solid is almost incompressible ($\nu \rightarrow 0.5$) because the strain in the thickness direction of the body can accommodate the incompressibility constraint.

Chapter 4

Coupling procedures for fluid flow-structural interaction problems

Consider a system composed of fluid and solid parts as shown in figure (4-1). We are interested in solving for the response of such a system. The first step is to choose an appropriate mathematical model to describe the behavior of the fluid and the structure. The next step is to couple the fluid and structural equations to obtain the response of the system.

Since problems in which viscous and convective effects are important are considered in this thesis, the Navier-Stokes equations are used to model the fluid. Different ways of solving the coupled (almost) incompressible Navier-Stokes and structural equations are described.

The chapter is organized as follows. A procedure to couple fluid flow and structural equations is presented and then the two main approaches used to solve fluid flow-structural interaction problems are described: the *simultaneous solution* and the *partitioned* procedures. A new scheme is introduced which has the advantage that it is unconditionally stable and that the unknowns are not solved all together but in each domain (fluid and structure) at a time, allowing us to separate the solution of the structural equations from the solution of the fluid flow system.

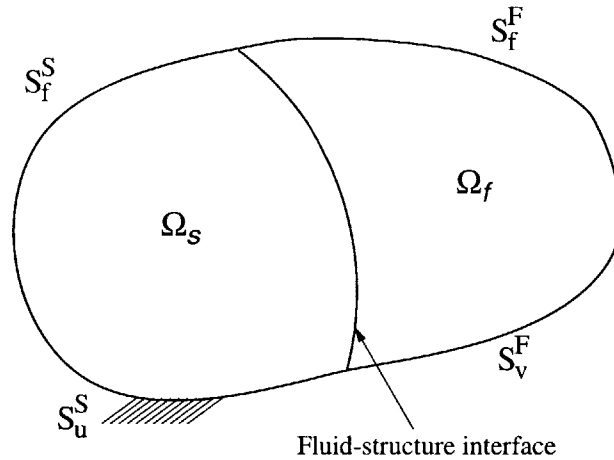


Figure 4-1: General fluid-structure interaction problem.

4.1 Coupling procedure

One of the most important characteristics of fluid flow-structural interaction problems is that the fluid domain can greatly change as a function of time. As a result, the ALE formulation of motion has to be used for the fluid-flow. Then, in addition to the calculation of the velocity and pressure fields, the mesh displacements have to be calculated.

In the analysis considered here, the same layers of elements (number and type) are used along the interface in the discretization of the fluid and structural domains. Hence, the force equilibrium conditions at the fluid flow-structural interface are directly satisfied through the element assemblage process. However, the compatibility conditions at the fluid flow-structural interface must be enforced since the fluid flow and structural variables are velocities and displacements respectively.

It is convenient to solve for the natural variables, displacements for structures and velocities for fluids. An advantage is that the same algorithm can be employed for both transient and steady state analysis. Also, natural variables are smoother than their time derivatives.

At the fluid flow-structural interface the particles that correspond to the fluid

and solid parts move together, i.e. they have the same displacements, velocities and accelerations. Therefore, in the ALE formulation the nodes at the interface should correspond to Lagrangian nodes. Assuming that no slip at the nodes of the fluid flow-structural interface is allowed, the *displacements* can be solved for *at the interface*, and these displacements can be used to calculate velocities at the interface (and hence the velocities of the fluid particles at the interface).

Since mesh displacements and velocities are calculated at the fluid-structure interface but can be arbitrarily specified otherwise, we can further assume that they are a linear function of fluid-structure interface displacements (and of the displacements of any other moving boundary or free surface),

$$\hat{\mathbf{u}} = \mathcal{L}(\mathbf{u}^I) \tag{4.1}$$

$$\hat{\mathbf{v}} = \mathcal{L}(\mathbf{v}^I) \tag{4.2}$$

where $\hat{\mathbf{u}}$ and $\hat{\mathbf{v}}$ are the mesh displacements and velocities respectively, \mathbf{u}^I and \mathbf{v}^I are the values of the displacements and velocities at the interface and \mathcal{L} is a linear operator. These interpolations, although not general, allow the solution of the example problems to be presented. In some cases, it can be necessary to allow some slip along the interface in order to preserve mesh regularity. In that case, the above equations are no longer valid and an additional equation governing the slip movement of the mesh at the interface must be provided. In what follows, the assumption that structure displacements coincide with nodal mesh displacements at the interface is used.

The linearized finite element matrix equations for the fluid, without including pressure terms explicitly (they are assumed to be contained in the variable vector \mathbf{v}) are

$$\begin{aligned} & \begin{pmatrix} \mathbf{M}_v^{II} & \mathbf{M}_v^{IF} \\ \mathbf{M}_v^{FI} & \mathbf{M}_v^{FF} \end{pmatrix} \begin{pmatrix} \dot{\mathbf{v}}^I \\ \dot{\mathbf{v}}^F \end{pmatrix} + \begin{pmatrix} \mathbf{K}_v^{II} + \hat{\mathbf{M}}_v^I \mathcal{L} & \mathbf{K}_v^{IF} \\ \mathbf{K}_v^{FI} + \hat{\mathbf{M}}_v^F \mathcal{L} & \mathbf{K}_v^{FF} \end{pmatrix} \begin{pmatrix} \mathbf{v}^I \\ \mathbf{v}^F \end{pmatrix} + \\ & \begin{pmatrix} \hat{\mathbf{K}}_v^I \mathcal{L} & \mathbf{0} \\ \hat{\mathbf{K}}_v^F \mathcal{L} & \mathbf{0} \end{pmatrix} \begin{pmatrix} \hat{\mathbf{u}}^I \\ \hat{\mathbf{u}}^F \end{pmatrix} = \begin{pmatrix} \mathbf{R}_f^I \\ \mathbf{R}_f^F \end{pmatrix} - \begin{pmatrix} \mathbf{F}_f^I \\ \mathbf{F}_f^F \end{pmatrix} \end{aligned} \quad (4.3)$$

where \mathbf{M}_v and \mathbf{K}_v are coefficient matrices of the linearized fluid equations, $\hat{\mathbf{M}}_v$ and $\hat{\mathbf{K}}_v$ are coefficient matrices from the ALE terms, \mathbf{v}^I and \mathbf{v}^F are the vectors of velocity increments corresponding to the fluid flow-structural interface and interior fluid nodes respectively, $\hat{\mathbf{u}}^I$ and $\hat{\mathbf{u}}^F$ are mesh displacement increments at the interface and interior nodes respectively, \mathbf{R}_f is the load vector corresponding to the fluid and \mathbf{F}_f contains the constant terms of the linearization. Equations (4.1) and (4.2) were assumed to hold in deriving equation (4.3). In what follows, for simplicity of notation, the linear operator \mathcal{L} is omitted (it is assumed to be contained in the matrices $\hat{\mathbf{M}}_v$ and $\hat{\mathbf{K}}_v$).

The finite element matrix equations corresponding to the linearized behavior of a general (nonlinear) structure are (neglecting damping effects)

$$\begin{pmatrix} \mathbf{M}_u^{SS} & \mathbf{M}_u^{SI} \\ \mathbf{M}_u^{IS} & \mathbf{M}_u^{II} \end{pmatrix} \begin{pmatrix} \ddot{\mathbf{u}}^S \\ \ddot{\mathbf{u}}^I \end{pmatrix} + \begin{pmatrix} \mathbf{K}_u^{SS} & \mathbf{K}_u^{SI} \\ \mathbf{K}_u^{IS} & \mathbf{K}_u^{II} \end{pmatrix} \begin{pmatrix} \mathbf{u}^S \\ \mathbf{u}^I \end{pmatrix} = \begin{pmatrix} \mathbf{R}_s^S \\ \mathbf{R}_s^I \end{pmatrix} - \begin{pmatrix} \mathbf{F}_s^S \\ \mathbf{F}_s^I \end{pmatrix} \quad (4.4)$$

where \mathbf{M}_u and \mathbf{K}_u are the mass and stiffness matrices corresponding to the structure, \mathbf{u}^I and \mathbf{u}^S are the vectors of displacement increments corresponding to the fluid-structure interface and interior structural nodes respectively; \mathbf{R}_s is the structure load vector and \mathbf{F}_s contains the constant terms of the linearization.

Assuming that no slip of nodes is allowed at the fluid-structure interface, $\mathbf{v}^I = \dot{\mathbf{u}}^I$ and $\dot{\mathbf{v}}^I = \ddot{\mathbf{u}}^I$ (continuity condition) and $\mathbf{R}_s^I + \mathbf{R}_f^I = \mathbf{0}$ (compatibility condition). Then, the *linearized* coupled fluid flow-structural equations can be expressed as

$$\mathbf{A}\ddot{\mathbf{U}} + \mathbf{B}\dot{\mathbf{U}} + \mathbf{C}\mathbf{U} = \mathbf{G} \quad (4.5)$$

where

$$\mathbf{A} = \begin{pmatrix} \mathbf{M}_u^{SS} & \mathbf{M}_u^{SI} & \mathbf{0} \\ \mathbf{M}_u^{IS} & \mathbf{M}_u^{II} + \mathbf{M}_v^{II} & \mathbf{M}_v^{IF} \\ \mathbf{0} & \mathbf{M}_v^{FI} & \mathbf{M}_v^{FF} \end{pmatrix} \quad (4.6)$$

$$\mathbf{B} = \begin{pmatrix} \mathbf{0} & \mathbf{0} & \mathbf{0} \\ \mathbf{0} & \mathbf{K}_v^{II} + \hat{\mathbf{M}}_v^I & \mathbf{K}_v^{IF} \\ \mathbf{0} & \mathbf{K}_v^{FI} + \hat{\mathbf{M}}_v^F & \mathbf{K}_v^{FF} \end{pmatrix} \quad (4.7)$$

$$\mathbf{C} = \begin{pmatrix} \mathbf{K}_u^{SS} & \mathbf{K}_u^{SI} & \mathbf{0} \\ \mathbf{K}_u^{IS} & \mathbf{K}_u^{II} + \hat{\mathbf{K}}_v^I & \mathbf{0} \\ \mathbf{0} & \hat{\mathbf{K}}_v^F & \mathbf{0} \end{pmatrix} \quad (4.8)$$

$$\mathbf{G} = \begin{pmatrix} \mathbf{R}_s^S - \mathbf{F}_s^S \\ -\mathbf{F}_f^I - \mathbf{F}_s^I \\ \mathbf{R}_f^F - \mathbf{F}_f^F \end{pmatrix} \quad (4.9)$$

and

$$\mathbf{u} = \begin{pmatrix} \mathbf{u}^S & \mathbf{u}^I & \mathbf{u}^F \end{pmatrix}^T \quad (4.10)$$

here \mathbf{u}^F are the displacement increments of the interior fluid particles, which are not calculated (see matrix \mathbf{C}), but instead, the fluid velocity increments are calculated (see matrix \mathbf{B}).

Solving for displacements at the interface, the coupling between fluid and structure becomes easy to perform.

Consider first the steady state case,

$$\ddot{\mathbf{u}}^S = \ddot{\mathbf{u}}^I = \ddot{\mathbf{u}}^F = \mathbf{0} \quad (4.11)$$

and

$$\dot{\mathbf{u}}^S = \dot{\mathbf{u}}^I = \mathbf{0} \quad (4.12)$$

Then, the steady state coupled fluid flow-structural equation (4.5) become,

$$\begin{pmatrix} \mathbf{K}_u^{SS} & \mathbf{K}_u^{SI} & \mathbf{0} \\ \mathbf{K}_u^{IS} & \mathbf{K}_u^{II} + \hat{\mathbf{K}}_v^I & \mathbf{K}_v^{IF} \\ \mathbf{0} & \hat{\mathbf{K}}_v^F & \mathbf{K}_v^{FF} \end{pmatrix} \begin{pmatrix} \mathbf{u}^S \\ \mathbf{u}^I \\ \mathbf{v}^F \end{pmatrix} = \begin{pmatrix} \mathbf{R}_s^S - \mathbf{F}_s^S \\ -\mathbf{F}_f^I - \mathbf{F}_s^I \\ \mathbf{R}_f^F - \mathbf{F}_f^F \end{pmatrix} \quad (4.13)$$

where \mathbf{v}^F is the vector of internal fluid velocity increments.

To solve for the transient fully coupled fluid flow-structural interaction response, time integration schemes need to be chosen. In this work, implicit time integration is used, and hence the time discretization can be written as follows (using a linear multistep method)

- Fluid (first order differential equation in time)

The time integration scheme has the form:

$${}^{t+\Delta t}\dot{v} = \alpha {}^{t+\Delta t}v + f ({}^t v, {}^t \dot{v}, \dots) \quad (4.14)$$

where α is a constant that depends on the specific time integration scheme employed and f is a linear function of the known velocities and accelerations at times t , $t - \Delta t$, $t - 2\Delta t$, ... With the equilibrium equations to be satisfied at time $t + \Delta t$ (for an implicit method), the linearized fluid flow equations can be written as

$$\mathbf{M}_v {}^{t+\Delta t}\dot{\mathbf{v}} + \mathbf{K}_v {}^{t+\Delta t}\mathbf{v} = {}^{t+\Delta t}\tilde{\mathbf{R}}_f \quad (4.15)$$

Solving for ${}^{t+\Delta t}\mathbf{v}$ gives

$$(\alpha \mathbf{M}_v + \mathbf{K}_v) {}^{t+\Delta t}\mathbf{v} = {}^{t+\Delta t}\tilde{\mathbf{R}}_f - \mathbf{M}_v \mathbf{f} ({}^t \mathbf{v}, {}^t \dot{\mathbf{v}}, \dots) \quad (4.16)$$

where ${}^{t+\Delta t}\tilde{\mathbf{R}}_f$ contains the load vector and the constant terms of the linearization.

- Structure (second order differential equation in time)

The time integration scheme has the form:

$${}^{t+\Delta t}\ddot{\mathbf{u}} = \beta {}^{t+\Delta t}\mathbf{u} + g({}^t\mathbf{u}, {}^t\dot{\mathbf{u}}, {}^t\ddot{\mathbf{u}}, \dots) \quad (4.17)$$

$${}^{t+\Delta t}\dot{\mathbf{u}} = \gamma {}^{t+\Delta t}\mathbf{u} + h({}^t\mathbf{u}, {}^t\dot{\mathbf{u}}, {}^t\ddot{\mathbf{u}}, \dots) \quad (4.18)$$

where β and γ are constants that depend on the actual integration time scheme employed and g and h are linear functions of the known displacements, velocities and accelerations at time t , $t - \Delta t$, $t - 2\Delta t$, ... Satisfying the equilibrium equations at time $t + \Delta t$ gives

$$\mathbf{M}_u {}^{t+\Delta t}\ddot{\mathbf{u}} + \mathbf{K}_u {}^{t+\Delta t}\mathbf{u} = {}^{t+\Delta t}\tilde{\mathbf{R}}_s \quad (4.19)$$

Solving for ${}^{t+\Delta t}\mathbf{u}$ results in

$$(\beta \mathbf{M}_u + \mathbf{K}_u) {}^{t+\Delta t}\mathbf{u} = {}^{t+\Delta t}\tilde{\mathbf{R}}_s - \mathbf{M}_u \mathbf{g}({}^t\mathbf{u}, {}^t\dot{\mathbf{u}}, {}^t\ddot{\mathbf{u}}, \dots) \quad (4.20)$$

where ${}^{t+\Delta t}\tilde{\mathbf{R}}_s$ contains known terms.

- Fluid flow-structural interface.

The time integration scheme has the form:

$${}^{t+\Delta t}v^I = \gamma {}^{t+\Delta t}u^I + h({}^t u^I, {}^t v^I, {}^t \dot{v}^I, \dots) \quad (4.21)$$

Note that here the same scheme is used as for the time integration of the displacements of the structure, see equation (4.18).

Introducing equation (4.21) into equation (4.16) and separating the unknowns corresponding to the interface from the internal fluid flow unknowns we obtain

$$\begin{pmatrix} \gamma(\alpha\mathbf{M}_v^{II} + \mathbf{K}_v^{II}) & \alpha\mathbf{M}_v^{IF} + \mathbf{K}_v^{IF} \\ \gamma(\alpha\mathbf{M}_v^{FI} + \mathbf{K}_v^{FI}) & \alpha\mathbf{M}_v^{FF} + \mathbf{K}_v^{FF} \end{pmatrix} \begin{pmatrix} \mathbf{u}^I \\ \mathbf{v}^F \end{pmatrix} = \begin{pmatrix} \check{\mathbf{R}}_f^I \\ \check{\mathbf{R}}_f^F \end{pmatrix} \quad (4.22)$$

where the load vector $\check{\mathbf{R}}_f$ contain the known terms of the linearization and time integration. Here, the contributions of the mesh movement to the fluid coefficient matrix are not shown explicitly.

The fluid flow and structural equations can now be coupled using equations (4.20) and (4.22), and the linearized fully coupled incremental fluid flow-structural interaction equation becomes

$$\begin{pmatrix} \bar{\mathbf{K}}_u^{SS} & \bar{\mathbf{K}}_u^{SI} & \mathbf{0} \\ \bar{\mathbf{K}}_u^{IS} & \bar{\mathbf{K}}_u^{II} + \bar{\mathbf{K}}_v^{II} & \bar{\mathbf{K}}_v^{IF} \\ \mathbf{0} & \bar{\mathbf{K}}_v^{FI} & \bar{\mathbf{K}}_v^{FF} \end{pmatrix} \begin{pmatrix} \mathbf{u}^S \\ \mathbf{u}^I \\ \mathbf{v}^F \end{pmatrix} = \begin{pmatrix} \check{\mathbf{R}}_s^S \\ \check{\mathbf{R}}^I \\ \check{\mathbf{R}}_f^F \end{pmatrix} \quad (4.23)$$

where from equation (4.20)

$$\begin{aligned} \bar{\mathbf{K}}_u^{SS} &= \beta\mathbf{M}_u^{SS} + \mathbf{K}_u^{SS} \\ \bar{\mathbf{K}}_u^{SI} &= \beta\mathbf{M}_u^{SI} + \mathbf{K}_u^{SI} \\ \bar{\mathbf{K}}_u^{IS} &= \beta\mathbf{M}_u^{IS} + \mathbf{K}_u^{IS} \\ \bar{\mathbf{K}}_u^{II} &= \beta\mathbf{M}_u^{II} + \mathbf{K}_u^{II} \end{aligned} \quad (4.24)$$

and from equation (4.22)

$$\begin{aligned} \bar{\mathbf{K}}_v^{II} &= \gamma(\alpha\mathbf{M}_v^{II} + \mathbf{K}_v^{II}) \\ \bar{\mathbf{K}}_v^{IF} &= \alpha\mathbf{M}_v^{IF} + \mathbf{K}_v^{IF} \\ \bar{\mathbf{K}}_v^{FI} &= \gamma(\alpha\mathbf{M}_v^{FI} + \mathbf{K}_v^{FI}) \\ \bar{\mathbf{K}}_v^{FF} &= \alpha\mathbf{M}_v^{FF} + \mathbf{K}_v^{FF} \end{aligned} \quad (4.25)$$

The variables corresponding to the fluid and the interface were defined above; $\check{\mathbf{R}}_s^S$ corresponds to the load vector of the internal structural degrees of freedom (including the known terms).

4.2 Different approaches for the solution of fluid-structure interaction problems

There are two main approaches that are used to solve fully coupled problems

- *Simultaneous* or *monolithic solution*: the equations are coupled and solved together;
- *Partitioned* or *block solution*: the system is divided into subsystems (corresponding to the fluid and structure domains), and each subsystem is solved separately. “Boundary conditions” at the fluid-structure interface act as coupling terms between the two subsystems.

4.2.1 Simultaneous solution

Using the simultaneous solution procedure, the coupled fluid flow and structural equations, (4.13) for a steady-state analysis or (4.23) for a transient analysis, are solved together and therefore the matrix equation to be solved contains all the unknowns (from the fluid and structure).

Since the fluid flow coefficient matrix is non-symmetric, when solving equations (4.13) or (4.23) using the simultaneous solution procedure, the complete fluid flow-structural interaction coefficient matrix is usually treated as non-symmetric. In addition, due to the nonlinear nature of the coupled system, the complete system of equations must be iterated upon until convergence is reached in each time step. This requires a large amount of calculations at each time step, and for large systems (of many degrees of freedom) the computer capacity and speed may rapidly become a constraint. However, using the simultaneous solution procedure unconditionally stable algorithms (for the linearized system) can be obtained by choosing appropriate time integration schemes for both the fluid flow and structural equations. For a stability analysis of the fully coupled fluid flow-structural interaction problem see chapter chapter 5.

4.2.2 Partitioned procedure

In the partitioned procedure the response of the coupled fluid flow-structural interaction system is calculated using already developed fluid flow and structural solvers. In this way, modularity is achieved and the complete system is divided into subsystems (corresponding to the fluid and structure, although subdivisions of them can also be considered). This approach allows the solution of larger systems and more flexibility in the selection of meshes for the fluid and structure.

Partitioned procedures for solving general coupled field problems have been studied together with accuracy and stability considerations, see [8] [9] [28]. A general partitioned procedure for fluid flow-structural interaction problems has been described in [5], [7].

The partitioned procedure consists of dividing the coefficient matrix of equations (4.13) or (4.23) into an implicit and an explicit part. The explicit part is put on the right hand side of the equilibrium equation and a predictor is applied to it. The equations are then solved factorizing the implicit part of the coefficient matrix.

In essence, the partitioned procedure can be thought of as a Gauss-Seidel iterative algorithm except that the predictor used can contain linear combinations of past solutions and their derivatives. Also, using partitioned procedures to solve a coupled equation, the coefficient matrix is partitioned in such a way that the equations from one field can be separated from the equations of the other field.

When dealing with fluid-structure interaction problems, the two fields, fluid and structure, have a common boundary, see figure (4-2). Denoting the two fields by x , y and the boundary by b , the coupled coefficient matrix can be written as

$$\mathbf{K} = \begin{pmatrix} \mathbf{K}_{xx} & \mathbf{K}_{xb} & \mathbf{0} \\ \mathbf{K}_{bx} & \mathbf{K}_{bb}^x + \mathbf{K}_{bb}^y & \mathbf{K}_{by} \\ \mathbf{0} & \mathbf{K}_{yb} & \mathbf{K}_{yy} \end{pmatrix} \quad (4.26)$$

The coefficient matrix, \mathbf{K} , is partitioned as $\mathbf{K} = \mathbf{K}_1 + \mathbf{K}_2$ where \mathbf{K}_1 is the implicit part of the matrix and \mathbf{K}_2 the explicit one (i.e. the predictor is applied to \mathbf{K}_2).

A useful partitioned procedure for fluid flow-structural interaction problems re-

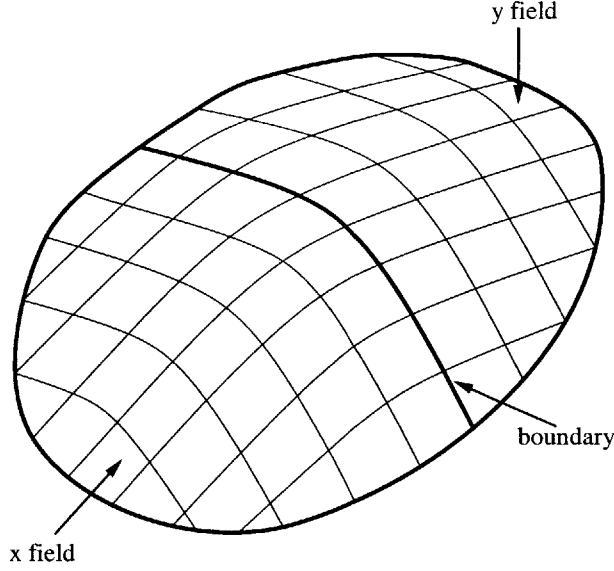


Figure 4-2: Finite element discretization of a fluid-structure interaction problem.

sults in the following partition of the coefficient matrix

$$\mathbf{K} = \begin{pmatrix} \mathbf{K}_{xx} & \mathbf{K}_{xb} & \mathbf{0} \\ \mathbf{K}_{bx} & \mathbf{K}_{bb}^x & \mathbf{K}_{by} \\ \mathbf{0} & \mathbf{0} & \mathbf{K}_{yy} \end{pmatrix} + \begin{pmatrix} \mathbf{0} & \mathbf{0} & \mathbf{0} \\ \mathbf{0} & \mathbf{K}_{bb}^y & \mathbf{0} \\ \mathbf{0} & \mathbf{K}_{yb} & \mathbf{0} \end{pmatrix} \quad (4.27)$$

where the first matrix is \mathbf{K}_1 , the implicit part, and the second is \mathbf{K}_2 , the explicit one. Since \mathbf{K}_{xx} and \mathbf{K}_{yy} are solved implicitly (i.e. they are part of \mathbf{K}_1), the algorithm corresponds to an implicit-implicit partitioned procedure.

Usually, structural solvers calculate displacements and viscous fluid solvers velocities, and then equations (4.3) and (4.4) can be used for the fluid and structure respectively in a partitioned procedure. Using equation (4.14) for the time integration, equation (4.3) becomes

$$\begin{pmatrix} \alpha \mathbf{M}_v^{II} + \mathbf{K}_v^{II} + \hat{\mathbf{M}}_v^I & \alpha \mathbf{M}_v^{IF} + \mathbf{K}_v^{IF} \\ \alpha \mathbf{M}_v^{FI} + \mathbf{K}_v^{FI} + \hat{\mathbf{M}}_v^F & \alpha \mathbf{M}_v^{FF} + \mathbf{K}_v^{FF} \end{pmatrix} \begin{pmatrix} \mathbf{v}^I \\ \mathbf{v}^F \end{pmatrix} + \begin{pmatrix} \hat{\mathbf{K}}_v^I & \mathbf{0} \\ \hat{\mathbf{K}}_v^F & \mathbf{0} \end{pmatrix} \begin{pmatrix} \hat{\mathbf{u}}^I \\ \hat{\mathbf{u}}^F \end{pmatrix} = \begin{pmatrix} \mathbf{R}_f^I - \tilde{\mathbf{F}}_f^I \\ \mathbf{R}_f^F - \tilde{\mathbf{F}}_f^F \end{pmatrix} \quad (4.28)$$

and using equation (4.17), equation (4.4) becomes

$$\begin{pmatrix} \beta \mathbf{M}_u^{SS} + \mathbf{K}_u^{SS} & \beta \mathbf{M}_u^{SI} + \mathbf{K}_u^{SI} \\ \beta \mathbf{M}_u^{SI} + \mathbf{K}_u^{SI} & \beta \mathbf{M}_u^{II} + \mathbf{K}_u^{II} \end{pmatrix} \begin{pmatrix} \mathbf{u}^S \\ \mathbf{u}^I \end{pmatrix} = \begin{pmatrix} \mathbf{R}_s^S - \tilde{\mathbf{F}}_s^S \\ \mathbf{R}_s^I - \tilde{\mathbf{F}}_s^I \end{pmatrix} \quad (4.29)$$

where $\tilde{\mathbf{F}}$ contains known terms from the linearization and time integration (the linear operator \mathcal{L} is assumed to be contained in the matrices $\hat{\mathbf{M}}$ and $\hat{\mathbf{K}}$ as before).

To solve the fully coupled fluid flow-structural interaction equations the following steps must be performed,

1. Calculate *predicted* displacement and velocity (incremental) values at the interface, $\bar{\mathbf{u}}^I$ and $\bar{\mathbf{v}}^I$, from the previous iteration (the predicted value can be just the value obtained in the last iteration or may be a linear combination of past solutions).
2. Solve the fluid equations (4.28) using the predicted velocities and displacements at the interface, that is to say solve

$$(\alpha \mathbf{M}_v^{FF} + \mathbf{K}_v^{FF}) \mathbf{v}^F = (\mathbf{R}_f^F - \tilde{\mathbf{F}}_f^F) - (\alpha \mathbf{M}_v^{FI} + \mathbf{K}_v^{FI} + \hat{\mathbf{M}}_v^F) \bar{\mathbf{v}}^I - \hat{\mathbf{K}}_v^F \bar{\mathbf{u}}^I \quad (4.30)$$

3. Using the calculated fluid velocity increments, \mathbf{v}^F , calculate the interface load vector that acts on the structure due to the fluid

$$\mathbf{R}_s^I = -\mathbf{R}_f^I = -[(\alpha \mathbf{M}_v^{IF} + \mathbf{K}_v^{IF}) \mathbf{v}^F + (\alpha \mathbf{M}_v^{II} + \mathbf{K}_v^{II} + \hat{\mathbf{M}}_v^I) \bar{\mathbf{v}}^I + \hat{\mathbf{K}}_v^I \bar{\mathbf{u}}^I + \tilde{\mathbf{F}}_f^I] \quad (4.31)$$

4. Calculate the structural response using the calculated load vector at the interface

$$\begin{pmatrix} \beta \mathbf{M}_u^{SS} + \mathbf{K}_u^{SS} & \beta \mathbf{M}_u^{SI} + \mathbf{K}_u^{SI} \\ \beta \mathbf{M}_u^{IS} + \mathbf{K}_u^{IS} & \beta \mathbf{M}_u^{II} + \mathbf{K}_u^{II} \end{pmatrix} \begin{pmatrix} \mathbf{u}^S \\ \mathbf{u}^I \end{pmatrix} = \begin{pmatrix} \mathbf{R}_s^S - \tilde{\mathbf{F}}_s^S \\ -\mathbf{R}_f^I - \tilde{\mathbf{F}}_s^I \end{pmatrix} \quad (4.32)$$

5. Iterate until convergence is achieved.

Putting all steps together in matrix notation and integrating $\bar{\mathbf{v}}^I$ using equation (4.21) we obtain

$$\begin{pmatrix} \beta\mathbf{M}_u^{SS} + \mathbf{K}_u^{SS} & \beta\mathbf{M}_u^{SI} + \mathbf{K}_u^{SI} & \mathbf{0} \\ \beta\mathbf{M}_u^{IS} + \mathbf{K}_u^{IS} & \beta\mathbf{M}_u^{II} + \mathbf{K}_u^{II} & \alpha\mathbf{M}_v^{IF} + \mathbf{K}_v^{IF} \\ \mathbf{0} & \mathbf{0} & \alpha\mathbf{M}_v^{FF} + \mathbf{K}_v^{FF} \end{pmatrix} \begin{pmatrix} \mathbf{u}_{i+1}^S \\ \mathbf{u}_{i+1}^I \\ \mathbf{v}_{i+1}^F \end{pmatrix} = \begin{pmatrix} \check{\mathbf{F}}^S \\ \check{\mathbf{F}}^I \\ \check{\mathbf{F}}^F \end{pmatrix} - \begin{pmatrix} \mathbf{0} & \mathbf{0} & \mathbf{0} \\ \mathbf{0} & \gamma(\alpha\mathbf{M}_v^{II} + \mathbf{K}_v^{II} + \hat{\mathbf{M}}_v^I) + \hat{\mathbf{K}}_v^I & \mathbf{0} \\ \mathbf{0} & \gamma(\alpha\mathbf{M}_v^{FI} + \mathbf{K}_v^{FI} + \hat{\mathbf{M}}_v^F) + \hat{\mathbf{K}}_v^F & \mathbf{0} \end{pmatrix} \begin{pmatrix} \bar{\mathbf{u}}_i^S \\ \bar{\mathbf{u}}_i^I \\ \bar{\mathbf{v}}_i^F \end{pmatrix} \quad (4.33)$$

where the subscripts $i, i + 1$ indicates fluid structure iteration step, and the vector $\check{\mathbf{F}}$ contains known terms.

Comparing equation (4.33) with equation (4.27), the partitioning performed on the coefficient matrix of the fully coupled system is evident.

If the coupled system is linear and the field equations symmetric, then, it was reported that on choosing an appropriate predictor, unconditionally stable implicit-implicit partitioned algorithms can be obtained with good accuracy characteristics without performing iterations at each time step [8] [9]. If the predictor is not good enough, iterations can be performed to achieve a better accuracy. These situations are referred to as loose (no iterations) and strong coupling. For a more general case, in which the system response is nonlinear, iterations are needed to converge with the nonlinear coupling terms. For a fluid flow-structural interaction problem in which the fluid is modeled using the Navier-Stokes equations unconditional stability is very difficult to assess and proposed partitioned algorithms are in fact conditionally stable.

4.3 Proposed scheme

Simultaneous solution and partitioned procedures have been used to solve fluid flow-structural interaction problems. However, as was mentioned before, improvements in these schemes are needed in order to obtain more robust, reliable and effective procedures. It is desirable to obtain an algorithm with the following characteristics:

1. unconditionally stable;
2. computationally efficient (in terms of amount of calculations performed in each time step);
3. useful for both dynamic and steady state analyses.

The proposed scheme satisfies all three requirements.

In the simultaneous solution procedure using equation (4.23) unconditional stability can be obtained by choosing appropriate time integration schemes. To increase the efficiency of the solution, we propose to solve equation (4.23) (or equation (4.13) in a steady-state analysis) by *condensing out the internal structural degrees of freedom prior to solving the system equations* at each time step (or load step).

Condensing out the internal structural degrees of freedom the following equations are obtained

$$\begin{pmatrix} \bar{\mathbf{K}}_u^{II} - \bar{\mathbf{K}}_u^{IS} (\bar{\mathbf{K}}_u^{SS})^{-1} \bar{\mathbf{K}}_u^{SI} + \bar{\mathbf{K}}_v^{II} & \bar{\mathbf{K}}_v^{IF} \\ \bar{\mathbf{K}}_v^{FI} & \bar{\mathbf{K}}_v^{FF} \end{pmatrix} \begin{pmatrix} \mathbf{u}^I \\ \mathbf{v}^F \end{pmatrix} = \begin{pmatrix} \check{\mathbf{R}}^I - \bar{\mathbf{K}}_u^{IS} (\bar{\mathbf{K}}_u^{SS})^{-1} \check{\mathbf{R}}_s^S \\ \check{\mathbf{R}}_f^F \end{pmatrix} \quad (4.34)$$

Equation (4.34) is completely equivalent to equation (4.23), but the unknowns to solve for in equation (4.34) correspond only to the *fluid flow degrees of freedom*. Since the fluid flow-structural interaction problem is nonlinear, equation (4.34) must be iterated upon in each time step until convergence of the solution is obtained. A Newton-Raphson iteration scheme is used for this purpose in this work [2].

Once the fluid flow response has been calculated using equation (4.34), the internal nodal point displacements of the structure are obtained using

$$\mathbf{u}^S = (\bar{\mathbf{K}}_u^{SS})^{-1} (\check{\mathbf{R}}_s^S - \bar{\mathbf{K}}_u^{SI} \mathbf{u}^I) \quad (4.35)$$

Equations (4.34) and (4.35) show that the proposed scheme conserves the unconditional stability and accuracy characteristics of the simultaneous solution procedure. At the same time the unknowns corresponding to the fluid flow and structural equations are solved separately. Of course, the calculated response contains all the effects of the fully coupled fluid flow-structural interaction problem.

The steps needed at each time step to calculate the response of the fluid flow-structural system are

1. Assemble the structural coefficient matrix and condense out the internal degrees of freedom (structural displacements other than the fluid flow-structural interface degrees of freedom).
2. Assemble the fluid flow coefficient matrix considering that the nodal motions at the fluid-structure interface are calculated as displacements (and therefore the time integration scheme for the displacements must be introduced in the fluid flow coefficient matrix), equation (4.22).
3. Add the condensed structural coefficient matrix (obtained in step 1) into the fluid flow coefficient matrix.
4. Solve the nonlinear equations obtained from step 3, equations (4.34).
5. Using the calculated displacements at the fluid-structure interface, calculate the internal displacements of the structure, equation (4.35).

If the structural equations are linear and a constant time step is used in transient analysis, then the constant matrices in equations (4.34) and (4.35), should be calculated only once, stored, and repeatedly used in steps 3 and 5. Also, since the structural coefficient matrix is symmetric a non-symmetric coefficient matrix is considered only in step 4 (i.e. when solving for the fluid response). If the structural equations were nonlinear the static condensation could be performed at each iteration or only in

certain intervals (with the requirement, of course, that the out-of-balance load vector is correctly calculated in each iteration) [2].

The number of iterations performed in each time step is given by the solution of equation (4.34) only (and (4.35) if the structural equations are nonlinear). If the structure is very compliant, convergence is reached more rapidly than in a partitioned procedure.

The disadvantage of the proposed scheme is that the bandwidth of the fluid flow matrix is increased due to the condensation of the internal structural degrees of freedom. Also, if the structure is very stiff, an ill-conditioned coefficient matrix for the coupled system can result, but in that case a partitioned procedure is probably more efficient and better used. Of course, the condensation of the structural degrees of freedom is not effective in case the contribution of the structure to the total number of degrees of freedom of the system is negligible.

Chapter 5

Stability analysis

A discussion of different time integration schemes can be found in [2] as well as a stability and accuracy analysis of them. Briefly, there are basically two types of schemes: explicit and implicit ones. The explicit schemes are usually faster per time step but a large number of time steps needs to be performed because they are *conditionally stable* (the time step required for stability must be smaller than a certain critical time step). On the other hand, in the implicit schemes the computational cost per time step is higher, but *unconditionally stable* schemes can be found, and the time step required need not be so small.

For a linear system, the solution vector at time $t + \Delta t$ can be expressed as

$${}^{t+\Delta t}\mathbf{X} = \mathbf{A} {}^t\mathbf{X} + {}^{t+\Delta t}\mathbf{F} \quad (5.1)$$

where \mathbf{A} is called the amplification matrix and ${}^{t+\Delta t}\mathbf{F}$ is a vector containing the effects of the boundary conditions (forces and applied displacements/velocities).

To analyze the stability of the time integration, we analyze equation (5.1) for the case in which the vector ${}^{t+\Delta t}\mathbf{F}$ is zero at all times (physically, the system is subject just to initial conditions). For this situation, the solution vector ${}^{t+\Delta t}\mathbf{X}$ must be bounded. Assuming that Δt does not change, after n timesteps we have

$${}^{n\Delta t}\mathbf{X} = \mathbf{A}^n {}^0\mathbf{X} \quad (5.2)$$

For ${}^{n\Delta t}\mathbf{X}$ to be bounded, the modulus of the maximum eigenvalue of the amplification matrix \mathbf{A} must be less than or equal to one (see for example [2]). In a conditionally stable scheme, this is true just for values of the time step Δt smaller than a critical time step Δt_{cr} , and in an unconditionally stable scheme, this is true for any time step size. For an incompressible or almost incompressible fluid, the time step limitations of explicit methods is very severe ($\Delta t_{cr} \sim 1/c$, where c is the sound velocity in the medium, which is ∞ for an incompressible fluid). Hence, implicit methods are used to solve the problem. Among those, unconditionally stable methods are of course preferred because they have no limitation on the time step size, the only limitation is given by accuracy considerations (and, in a nonlinear problem, convergence of the iterative algorithm employed).

5.1 Linearized fluid flow equations

A stability analysis, can only be performed on a *linear system*. So let us take the simplest case of a viscous linear fluid to analyze the stability of a time integration scheme for the fluid flow: the Stokes problem. In the Stokes problem, the fluid is assumed to be fully incompressible and in addition, the convective terms are neglected, leading to a system of equations of the form

$$\begin{pmatrix} \mathbf{M}_{vv} & \mathbf{0} \\ \mathbf{0} & \mathbf{0} \end{pmatrix} \begin{pmatrix} {}^{t+\Delta t}\dot{\mathbf{v}} \\ {}^{t+\Delta t}\dot{\mathbf{p}} \end{pmatrix} + \begin{pmatrix} \mathbf{K}_{vv} & \mathbf{K}_{vp} \\ \mathbf{K}_{vp}^T & \mathbf{0} \end{pmatrix} \begin{pmatrix} {}^{t+\Delta t}\mathbf{v} \\ {}^{t+\Delta t}\mathbf{p} \end{pmatrix} = \begin{pmatrix} {}^{t+\Delta t}\mathbf{R}_f \\ \mathbf{0} \end{pmatrix} \quad (5.3)$$

where the superscript T indicates transpose and \mathbf{v} and \mathbf{p} are the actual velocities and pressures. The matrices \mathbf{M}_{vv} and \mathbf{K}_{vv} are constant and symmetric, and \mathbf{K}_{vp} is constant.

Let us assume that the columns of the matrix \mathbf{Q} contain the basis vectors of the null space of \mathbf{K}_{vp}^T . Then,

$$\mathbf{K}_{vp}^T \mathbf{Q} = \mathbf{0} \quad (5.4)$$

and because $\mathbf{K}_{vp}^T \mathbf{v} = \mathbf{0}$, we can express \mathbf{v} as

$$\mathbf{v} = \mathbf{Q}\mathbf{V} \quad (5.5)$$

Using this change of variables into equation (5.3), and multiplying by \mathbf{Q}^T , (taking into account that \mathbf{Q} does not change in time because \mathbf{K}_{vp}^T is constant) the following equation is obtained

$$\mathbf{Q}^T \mathbf{M}_{vv} \mathbf{Q} \dot{\mathbf{V}} + \mathbf{Q}^T \mathbf{K}_{vv} \mathbf{Q} \mathbf{V} = \mathbf{0} \quad (5.6)$$

This equations can be re-written as

$$\mathbf{B} \dot{\mathbf{V}} + \mathbf{D} \mathbf{V} = \mathbf{0} \quad (5.7)$$

where \mathbf{B} and \mathbf{D} are positive definite matrices. If we look for solutions of the type $U = e^{-\lambda t}$, the following generalized eigenproblem is obtained

$$\mathbf{D} \phi = \lambda \mathbf{B} \phi \quad (5.8)$$

By choosing D-orthonormal eigenvectors, the problem is decoupled and a system of single degree of freedom equations is obtained

$$\dot{v}_i + \lambda_i v_i = 0 ; \quad i = 1, \dots, n \quad (5.9)$$

Therefore, the n coupled equations of (5.7) are equivalent to n single degree of freedom equations of the form (5.9). The stability analysis can then be performed on a single degree of freedom equation.

In this thesis the trapezoidal rule, Euler backward and Gear's time integration schemes, which are unconditionally stable when applied to equation (5.9), are considered for the fluid flow equations.

5.2 Linear structural equations

The displacement based finite element equations of motion of a linear (or linearized) structure can be written as

$$\mathbf{M}_u {}^{t+\Delta t}\ddot{\mathbf{u}} + \mathbf{K}_u {}^{t+\Delta t}\mathbf{u} = {}^{t+\Delta t}\mathbf{R}_u \quad (5.10)$$

If we look for solutions of the type $u = e^{-i \omega t}$, the following generalized eigenproblem is obtained

$$\omega^2 \mathbf{M}_u \phi = \mathbf{K}_u \phi \quad (5.11)$$

By choosing M-orthonormal eigenvectors, the problem is decoupled and the system of single degree of freedom equations obtained is

$$\ddot{x}_i + \omega_i^2 x_i = 0 ; \quad i = 1, \dots, n \quad (5.12)$$

Then, the stability of the system can be assessed from a single degree of freedom equation. For the displacement/pressure formulation, a similar procedure as that employed for the fluid equations can be performed, and the equations can be decoupled into single degree of freedom equations of the form (5.12).

In this thesis the trapezoidal rule, which is unconditionally stable and second order accurate in time when applied to equation (5.12), is employed to solve for the time response of the structural equations.

5.3 Fluid-flow structural interaction equations

When solving a fluid flow-structural interaction problem, unconditionally stable algorithms are desirable because it is important to be able to distinguish between physical instabilities and numerical ones.

5.3.1 Partitioned procedures

When using implicit-implicit partitioned procedures, one looks for an unconditionally stable scheme. However, the stability of the partitioned procedure is usually difficult to assess. In [8] and [9], a general theory of partitioned procedures, including the stability and accuracy of each of them was developed for linear structure-structure interaction problems. There, it was shown that the predictors play an important role, not only regarding the stability of the procedures but also for the accuracy.

One of the principal drawbacks of the partitioned method is that although the equations in each field are integrated using unconditionally stable time integration schemes, the iterative procedure is usually *conditionally stable*. Some stabilization techniques were considered in [4] for a particular type of fluid structure interaction problem (in which both the fluid and structural coefficient matrices are symmetric and the equations are linear). However, an unconditionally stable partitioned procedure for the solution of the coupled (almost) incompressible Navier-Stokes equations and structural equations is not yet available.

5.3.2 Proposed scheme

In this section, the stability of the coupled system (4.23) is considered, and in particular a stability analysis is performed for the case in which the *trapezoidal rule* is used for the structure, and the *trapezoidal rule* and *Gear's time integration* schemes (both second order accurate in time) and the *Euler backward method* are used for the fluid. The analysis performed here is by no means complete but is presented to give some insight into the scheme used.

Stability considerations regarding the combination of time integration schemes for the fluid and structure are also applicable to partitioned procedures because they use in general different time integration schemes for the fluid and structural fields and in addition partitioned procedures must converge to the solution of the simultaneous solution procedure.

Consider equations (5.3) and (5.10) at the interface, where then \mathbf{R}_f and \mathbf{R}_u are

the load vectors corresponding to the forces exerted by the structure over the fluid and viceversa. The equilibrium condition at the interface is

$$\mathbf{R}_f + \mathbf{R}_u = \mathbf{0} \quad (5.13)$$

Let us assume, as before, that the columns of the matrix \mathbf{Q} contain the basis vectors of the null space of \mathbf{K}_{vp}^T . Then,

$$\mathbf{v} = \mathbf{Q} \mathbf{V} \quad (5.14)$$

Also, since $\dot{\mathbf{u}} = \mathbf{v}$ at the interface

$$\mathbf{u} = \mathbf{Q} \mathbf{U} \quad (5.15)$$

Using this change of variables in equations (5.3) and (5.10), pre-multiplying by \mathbf{Q}^T and using equation (5.13), we obtain

$$\mathbf{M}_u^* \ddot{\mathbf{U}} + \mathbf{K}_u^* \mathbf{U} + \mathbf{M}_v^* \dot{\mathbf{V}} + \mathbf{K}_v^* \mathbf{V} = \mathbf{0} \quad (5.16)$$

where

$$\begin{aligned} \mathbf{M}_u^* &= \mathbf{Q}^T \mathbf{M}_u \mathbf{Q} \\ \mathbf{K}_u^* &= \mathbf{Q}^T \mathbf{K}_u \mathbf{Q} \\ \mathbf{M}_v^* &= \mathbf{Q}^T \mathbf{M}_{vv} \mathbf{Q} \\ \mathbf{K}_v^* &= \mathbf{Q}^T \mathbf{K}_{vv} \mathbf{Q} \end{aligned} \quad (5.17)$$

Based on equation (5.16), a single degree of freedom equation at the interface can now be considered

$${}^{t+\Delta t}\ddot{x} + m {}^{t+\Delta t}\dot{v} + \lambda {}^{t+\Delta t}v + \omega^2 {}^{t+\Delta t}x = 0 \quad (5.18)$$

where x and v are structural and fluid variables respectively (displacements and velocities). We test the integration schemes for stability using this equation.

Use of trapezoidal rule for the fluid

If the trapezoidal rule is used for both the structure and fluid flow equations

$${}^{t+\Delta t}\dot{x} = {}^{t+\Delta t}v \quad (5.19)$$

$${}^{t+\Delta t}\ddot{x} = {}^{t+\Delta t}\dot{v} \quad (5.20)$$

and equation (5.18) becomes

$$(1 + m) {}^{t+\Delta t}\ddot{x} + \lambda {}^{t+\Delta t}\dot{x} + \omega^2 {}^{t+\Delta t}x = 0 \quad (5.21)$$

Dividing by $(1 + m)$, and using $\bar{\lambda} = \frac{\lambda}{1+m}$, $\bar{\omega} = \frac{\omega}{\sqrt{1+m}}$

$${}^{t+\Delta t}\ddot{x} + \bar{\lambda} {}^{t+\Delta t}\dot{x} + \bar{\omega}^2 {}^{t+\Delta t}x = 0 \quad (5.22)$$

Equation (5.18) is identical to an uncoupled one degree of freedom structural equation (taking $\bar{\lambda} = 2\xi\bar{\omega}$, where ξ is the damping ratio). Since the trapezoidal rule is unconditionally stable for this equation, it is also unconditionally stable for the coupled single degree of freedom equation (5.18).

This seems to be an ideal time integration choice: the accelerations are calculated in the same way in both the fluid and structure (this is not true for other combinations of time integration procedures). Moreover, the trapezoidal rule applied to a first order differential equation can be classified as a linear multistep method of first order. A theorem due to Dahlquist states that an LMS method is at most second order accurate (in time) and the second order accurate method with the smallest constant is the trapezoidal rule [29]. As a consequence, the trapezoidal rule seems to be the better choice for the fluid. However, using the trapezoidal scheme, spurious oscillations may occur in the solution [2]. This response can be seen from the time discretization of the velocity

$${}^{t+\Delta t}\dot{v} = \frac{2}{\Delta t} \left({}^{t+\Delta t}v - {}^t v \right) - {}^t\dot{v} \quad (5.23)$$

applied to the one degree of freedom first order equation

$${}^{t+\Delta t}\dot{v} + \lambda {}^{t+\Delta t}v = 0 \quad (5.24)$$

Substitution of (5.23) onto (5.24) leads to

$${}^{t+\Delta t}v = \frac{1 - 0.5 \lambda \Delta t}{1 + 0.5 \lambda \Delta t} {}^t v \quad (5.25)$$

Therefore if $\lambda \Delta t > 2$ oscillations occur. To avoid these oscillations, another time integration scheme must be used. The scheme incorporates some artificial damping in the high frequency modes (responsible for the oscillations in the trapezoidal rule) while conserving good accuracy properties at the low frequencies.

Use of Gear's method for the fluid

A second-order accurate unconditionally stable method that produces less oscillations in the solution is due to Gear [30]. Gear's time integration scheme is a second order linear multistep method

$${}^{t+\Delta t}\dot{v} = \frac{1}{\Delta t} \left(\frac{3}{2} {}^{t+\Delta t}v - 2 {}^t v + \frac{1}{2} {}^{t-\Delta t}v \right) \quad (5.26)$$

Consider the stability of equation (5.18) when the trapezoidal rule is used for the structural equations and Gear's time integration scheme for the fluid.

Using the trapezoidal rule for the structure, we have

$$\frac{2}{\Delta t} {}^{t+\Delta t}x - {}^{t+\Delta t}\dot{x} = \frac{2}{\Delta t} {}^t x + {}^t \dot{x} \quad (5.27)$$

$$\frac{4}{\Delta t^2} {}^{t+\Delta t}x - {}^{t+\Delta t}\ddot{x} = \frac{4}{\Delta t^2} {}^t x + \frac{4}{\Delta t} {}^t \dot{x} + {}^t \ddot{x} \quad (5.28)$$

Substituting equations (5.28) and (5.26) into (5.18) and taking into account that the fluid velocities ${}^{t+\Delta t}v = {}^{t+\Delta t} \dot{x}$ are calculated using equation (5.27) (because in the proposed fluid-structure interaction scheme displacements are calculated at the

interface), the following equation is obtained

$$\begin{aligned} & \left(\frac{4}{\Delta t^2} + \omega^2 \right) {}^{t+\Delta t}x + \left(\frac{3m}{2\Delta t} + \lambda \right) {}^{t+\Delta t}\dot{x} = \\ & \frac{4}{\Delta t^2} {}^t x + \left(\frac{4}{\Delta t} + \frac{2m}{\Delta t} \right) {}^t\dot{x} - \frac{m}{2\Delta t} {}^{t-\Delta t}\dot{x} + {}^t\ddot{x} \end{aligned} \quad (5.29)$$

Then, using equations (5.27), (5.28) and (5.29), equation (5.18) can be expressed as

$${}^{t+\Delta t}\mathbf{X} = \mathbf{A} {}^t\mathbf{X} \quad (5.30)$$

where

$${}^{t+\Delta t}\mathbf{X} = \begin{pmatrix} {}^{t+\Delta t}x \\ {}^{t+\Delta t}\dot{x} \equiv {}^{t+\Delta t}v \\ {}^t\dot{x} \equiv {}^tv \\ {}^{t+\Delta t}\ddot{x} \end{pmatrix} \text{ and } {}^t\mathbf{X} = \begin{pmatrix} {}^tx \\ {}^t\dot{x} \\ {}^{t-\Delta t}\dot{x} \\ {}^t\ddot{x} \end{pmatrix}$$

and the amplification matrix \mathbf{A} is given by

$$\mathbf{A} = \frac{1}{F} \begin{pmatrix} 4 + 2\Delta t\lambda + 3m & \Delta t(4 + \Delta t\lambda + 3.5m) & -\Delta t m & \Delta t^2 \\ -2\Delta t\omega^2 & 4 + 4m - \Delta t^2\omega^2 & -m & 2\Delta t \\ 0 & F & 0 & 0 \\ -4\omega^2 & 2m/\Delta t - 4(\lambda + \Delta t\omega^2) & -2m/\Delta t & -(2\Delta t\lambda + 3m + \Delta t^2\omega^2) \end{pmatrix} \quad (5.31)$$

with $F = 4 + 3m + \Delta t^2\omega^2 + 2\Delta t\lambda$

For stability, we need

$$\rho(\mathbf{A}) = \max |\lambda_i| \leq 1 \quad (5.32)$$

where λ_i are the eigenvalues of \mathbf{A} , $\lambda_i = \lambda_i(\omega\Delta t, \lambda\Delta t, m)$, and $\rho(\mathbf{A})$ is the spectral radius of \mathbf{A} .

The eigenvalues of \mathbf{A} are the roots of the fourth-order characteristic polynomial $p(s) = 0$. However, we just need to know if the roots of the characteristic polynomial

are, in modulus, less than or equal to one, and therefore if they lie inside of a unit circle with center in 0. The transformation

$$s = \frac{1+z}{1-z} \quad (5.33)$$

maps the interior of the unit circle into the region $Re(z) < 0$ and the contour of the unit circle into the imaginary axis. This can be seen as follows. From equation (5.33) we have

$$z = \frac{s-1}{s+1} \quad (5.34)$$

Setting $s = r e^{i\theta} = r \cos(\theta) + i r \sin(\theta)$, and substituting into equation (5.34) we get

$$z = \frac{r \cos(\theta) + i r \sin(\theta) - 1}{r \cos(\theta) + i r \sin(\theta) + 1} = \frac{r^2 - 1 + i r \sin(\theta)}{[r \cos(\theta) + 1]^2 + r^2 \sin^2(\theta)} \quad (5.35)$$

Since the denominator of equation (5.35) is always positive, the real part of z is negative if $|\lambda| = r < 1$.

Applying the mapping (5.33) to $p(s)$, another polynomial is obtained, $\tilde{p}(z)$, given by

$$\tilde{p}(z) = a_0 + a_1 z + a_2 z^2 + a_3 z^3 + a_4 z^4 \quad (5.36)$$

where

$$\begin{aligned} a_0 &= \Delta t^2 \omega^2 \\ a_1 &= 2 \Delta t^2 \omega^2 + 2 \Delta t \lambda \\ a_2 &= \Delta t^2 \omega^2 + 4 \Delta t \lambda + 4 m + 4 \\ a_3 &= 2 \Delta t \lambda + 8 m + 8 \\ a_4 &= 4 \end{aligned} \quad (5.37)$$

Using the Routh-Hurwitz criterion (see for example [31]) for $\tilde{p}(z)$, the stability of the coupled system can be assessed. For this fourth-order system, the Routh-Hurwitz criterion establishes that for the roots of $\tilde{p}(z)$ to lie in the region $Re(z) \leq 0$, the

coefficients of $\tilde{p}(z)$ must be all positive, and in addition

$$a_2 a_3 - a_1 a_4 > 0 \quad (5.38)$$

$$-a_0 a_3^2 - a_1^2 a_4 + a_1 a_2 a_3 > 0 \quad (5.39)$$

These conditions are satisfied for $\tilde{p}(z)$, and therefore using Gear's method for the fluid and the trapezoidal rule for the structure in equation (5.18) an unconditionally stable scheme is obtained.

Use of the Euler backward method for the fluid

The procedure described above can be applied to the case in which the Euler backward method is used for the time integration of the fluid flow and the trapezoidal rule for the structure. The Euler backward method is unconditionally stable and first-order accurate in time. It is given by the following expression,

$${}^{t+\Delta t} \dot{v} = \frac{1}{\Delta t} ({}^{t+\Delta t} v - {}^t v) \quad (5.40)$$

Substituting equations (5.28) and (5.40) into (5.18) and taking into account that the fluid velocities ${}^{t+\Delta t} v = {}^{t+\Delta t} \dot{x}$ are calculated using (5.27), the following equation is obtained

$$\begin{aligned} \left(\frac{4}{\Delta t^2} + \omega^2 \right) {}^{t+\Delta t} x + \left(\frac{m}{\Delta t} + \lambda \right) {}^{t+\Delta t} \dot{x} = \\ \frac{4}{\Delta t^2} {}^t x + \left(\frac{4}{\Delta t} + \frac{m}{\Delta t} \right) {}^t \dot{x} + {}^t \ddot{x} \end{aligned} \quad (5.41)$$

Then, using equations (5.27), (5.28) and (5.41), equation (5.18) can be expressed as

$${}^{t+\Delta t} \mathbf{X} = \mathbf{A} {}^t \mathbf{X} \quad (5.42)$$

where here

$${}^{t+\Delta t}\mathbf{X} = \begin{pmatrix} {}^{t+\Delta t}x \\ {}^{t+\Delta t}\dot{x} \equiv {}^{t+\Delta t}v \\ {}^{t+\Delta t}\ddot{x} \end{pmatrix} \text{ and } {}^t\mathbf{X} = \begin{pmatrix} {}^tx \\ {}^t\dot{x} \\ {}^t\ddot{x} \end{pmatrix} \quad (5.43)$$

and the amplification matrix \mathbf{A} is given by

$$\mathbf{A} = \frac{1}{F} \begin{pmatrix} 4 + 2 \Delta t \lambda + 2 m & \Delta t(4 + \Delta t \lambda + 2m) & \Delta t^2 \\ -2\Delta t\omega^2 & 4 + 2m - \Delta t^2\omega^2 & 2\Delta t \\ -4\omega^2 & -4(\lambda + \Delta t\omega^2) & -(2\Delta t \lambda + 2m + \Delta t^2\omega^2) \end{pmatrix} \quad (5.44)$$

with $F = 4 + 2 m + \Delta t^2\omega^2 + 2\Delta t \lambda$

Applying the transformation given by equation (5.33) to the characteristic polynomial of this amplification matrix, the following third-order polynomial is obtained

$$\tilde{p}(z) = b_0 + b_1z + b_2z^2 + b_3z^3 \quad (5.45)$$

where

$$\begin{aligned} b_0 &= \Delta t^2 \omega^2 \\ b_1 &= \Delta t^2 \omega^2 + 2 \Delta t \lambda \\ b_2 &= 2 \Delta t \lambda + 4 m + 4 \\ b_3 &= 4 \end{aligned} \quad (5.46)$$

For this third-order system, the Routh-Hurwitz criterion establishes that for the roots of $\tilde{p}(z)$ to lie in the region $Re(z) \leq 0$, the coefficients of $\tilde{p}(z)$ must be all positive, and in addition

$$b_1 b_2 - b_3 b_0 > 0 \quad (5.47)$$

These conditions are satisfied and therefore using the Euler backward method for the fluid and the trapezoidal rule for the structure in equation (5.18) an unconditionally stable scheme is obtained.

Chapter 6

Example solutions

The proposed algorithm, described in chapter 4, was implemented in a computer program. In this chapter, the solution of two fluid flow-structural interaction problems solved using the proposed scheme are given. The examples were chosen to demonstrate the capabilities of the proposed scheme. In both of them the structure is very compliant and therefore a large number of iterations is required to solve the fully coupled problem using partitioned procedures. The structure is assumed to have a linear response. The examples were taken from biomechanical applications, where similar problems are solved to understand the behavior of blood flow in veins and arteries.

6.1 Analysis of pressure wave propagation in a tube

The type of problem solved here is encountered, for example, in the analysis of pressure pulse propagations in blood vessels [32].

The system considered is shown in figure 6-1. It consists of an axisymmetric tube filled with a viscous fluid initially at rest.

The fluid properties employed for this problem are as follows:

viscosity, $\mu = 0.005 \text{ kg/m s}$;

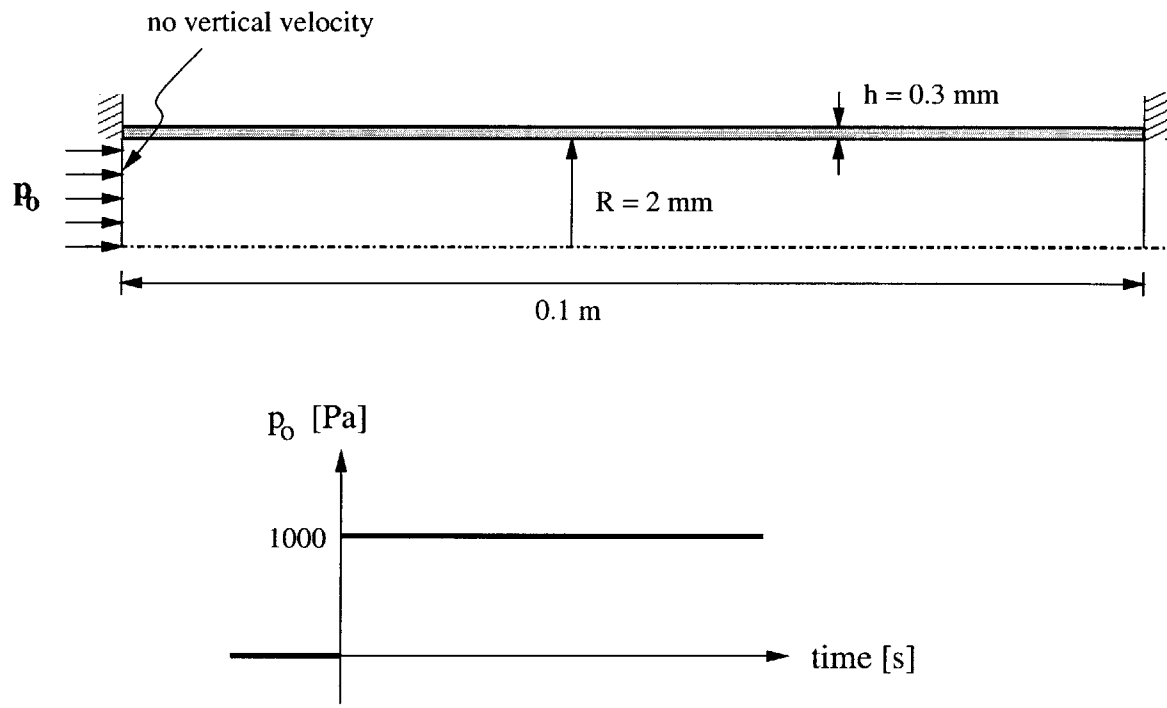


Figure 6-1: Pressure wave propagation problem. Geometry and boundary conditions considered.

density, $\rho_F = 1000 \text{ kg/m}^3$;

bulk modulus, $\kappa = 2.25 \cdot 10^7 \text{ N/m}^2$.

The tube properties are:

Young's modulus, $E = 2 \cdot 10^5 \text{ N/m}^2$;

density, $\rho_S = 1000 \text{ kg/m}^3$;

Poisson's ratio, $\nu = 0.4$.

The fluid domain was discretized using a 100 by 5 uniform mesh of 9/3 elements [2]. For the structural domain a 100 by 1 uniform mesh consisting of 9/3 elements was employed. Small displacements for the structure were assumed. The trapezoidal rule was employed for the time integration of the structural equations whereas the Euler backward method was used in the time integration of the fluid-flow equations [2]. If the trapezoidal rule is used for the fluid, some artificial oscillations between two consecutive time steps are observed.

Figure 6-2 shows the calculated pressure of the fluid along the tube centerline at different times. It is seen that a pressure wave propagates along the tube and that its amplitude decreases with distance from the tube inlet, due to viscous effects. In figure 6-3 the deformation of the tube due to the pressure wave and the fluid velocities inside the tube are shown, all for time 0.01 sec.

A simple analytical model of the pressure wave propagation problem can be obtained by assuming that the fluid is inviscid and incompressible, the fluid pressure is only a function of the transverse tube area, and the fluid velocity is much smaller than the speed of propagation of the pressure wave [33], see the Appendix. With these assumptions, the pressure wave speed is found to be

$$c = \sqrt{\frac{E h}{2 R \rho_F}} \quad (6.1)$$

where h is the tube thickness and R is the undeformed tube radius (see figure 6-1).

Equation (6.1) is the Moens-Korteweg wave speed, $c = 3.87 \text{ m/s}$ for the problem considered here. For the finite element solution (figure 6-2), the wave speed is $c = 3.48 \text{ m/s}$, and hence about 10% lower. This difference is largely due to the simplified

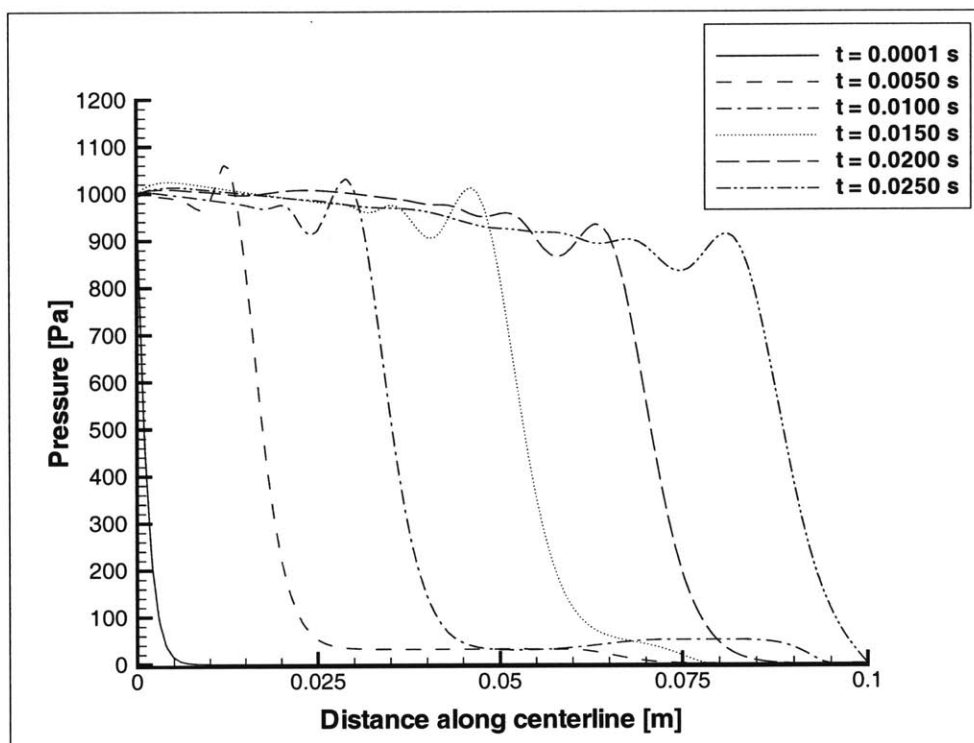


Figure 6-2: Calculated pressure along the tube centerline for different instants of time, for the pressure wave propagation problem.

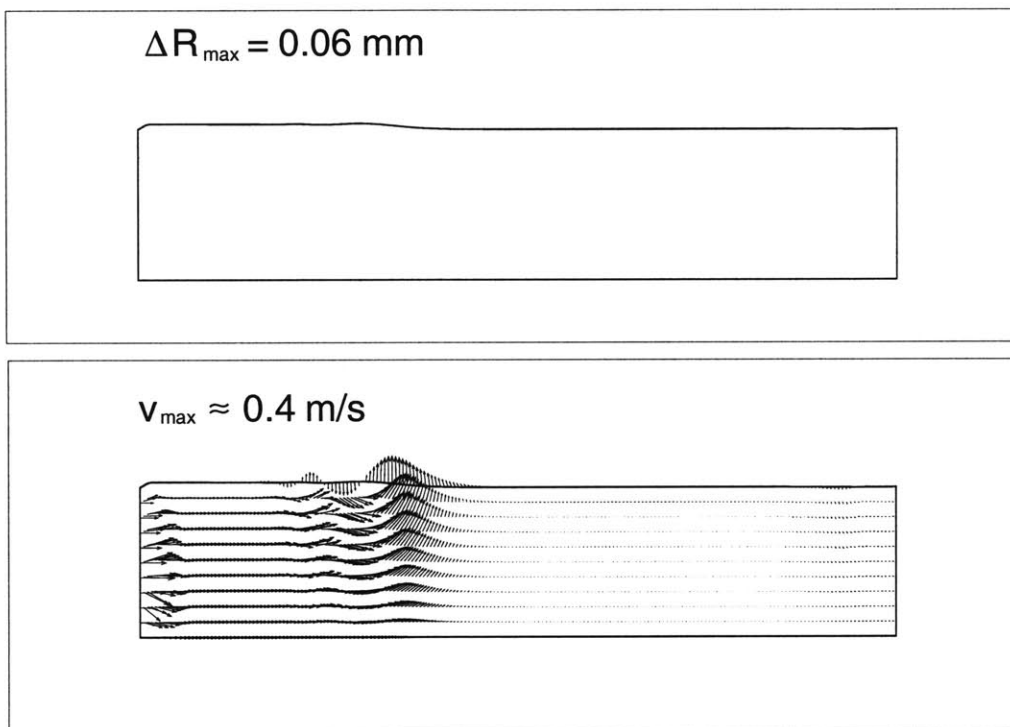


Figure 6-3: Deformation of tube and fluid velocities inside the tube due to pressure wave at $t = 0.01 \text{ sec}$. Radius enlarged 10 times.

assumptions in the analytical model.

It is interesting to note that if the same problem is solved using the partitioned procedure described in section 4.2.2, then not only many iterations are needed to converge (i.e. iterations between the field codes) but also the time step required for convergence is inversely proportional to the bulk modulus of the fluid. Thus, convergence is not achieved if the fluid is modeled as incompressible. This problem, however, is not observed when using the proposed scheme (equivalent to a simultaneous solution procedure). However, the mentioned convergence difficulties are not related to the stability of the partitioned procedure but to the solution of the nonlinear problem. In a general nonlinear problem the iterative procedure converges only if the start-up solution “guess” is close enough to the actual solution. Similarly, when solving a nonlinear coupled problem using partitioned procedures, the fluid solution obtained at the beginning (assuming that the iterative procedure does start with the fluid flow equations) may be far from the actual coupled solution, and as a consequence the iterative procedure may diverge. For the particular case considered here, the initial fluid solution of an incompressible fluid inside a rigid tube with a pressure difference between the tube ends corresponds to the Poiseuille flow, which is clearly far from the actual solution of the coupled problem.

6.2 Analysis of collapsible channel

The second example considered consists of a two-dimensional channel in which a part of the top wall is replaced by a collapsible segment plus a segment that can displace in the horizontal direction only as shown in figure 6-4. This type of problem is of interest in the study of the collapse behavior of blood vessels [33], [34], [35].

The channel is filled with a viscous fluid at rest. At time $t = 0$, the normal traction at the outlet of the tube is decreased as shown in figure 6-4. The pressure difference between the channel inlet and outlet starts to move the fluid inside the channel, and since the pressure below the collapsible segment is less than the pressure above it, the segment starts to move downward.

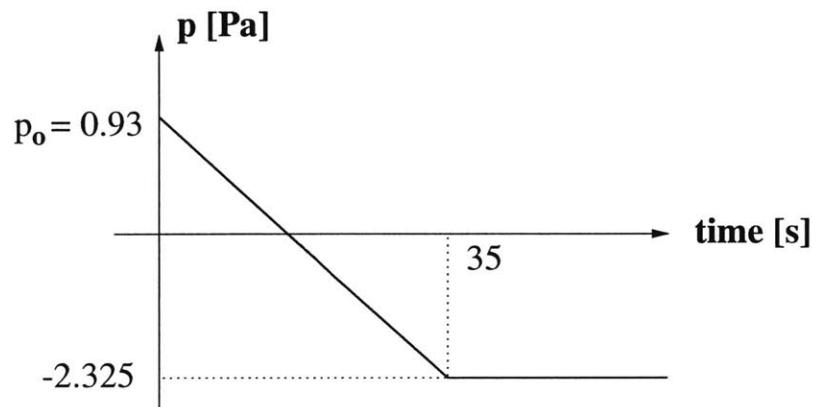
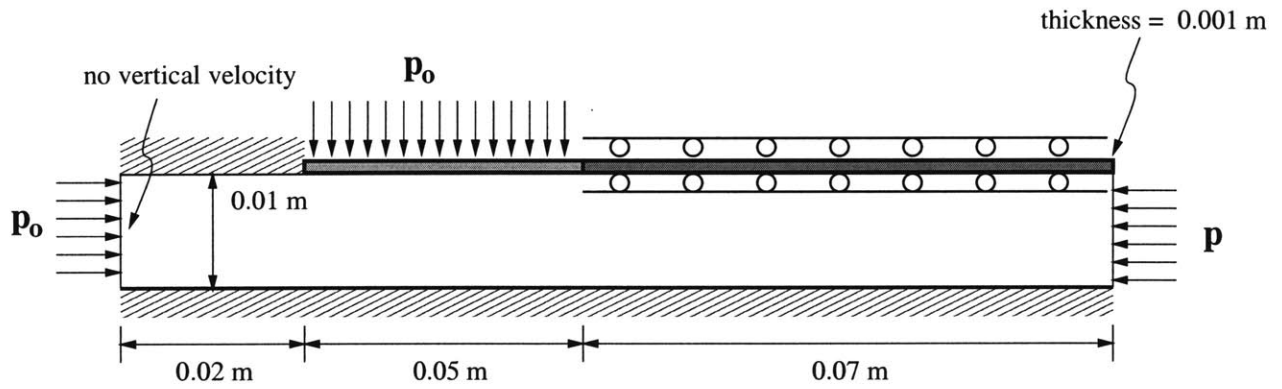


Figure 6-4: Collapsible channel problem. Geometry and boundary conditions considered.

The fluid properties employed for this problem are:

$$\mu = 0.002 \text{ kg/m s};$$

$$\rho_F = 1000 \text{ kg/m}^3;$$

$$\kappa = 2.1 \cdot 10^9 \text{ N/m}^2.$$

The collapsible segment properties are:

$$E = 2 \cdot 10^5 \text{ N/m}^2;$$

$$\rho_S = 1000 \text{ kg/m}^3;$$

$$\nu = 0.2.$$

The properties of the segment that can only displace horizontally are:

$$E = 2 \cdot 10^5 \text{ N/m}^2;$$

$$\rho_S = 1 \text{ kg/m}^3;$$

$$\nu = 0.3.$$

The fluid domain was discretized using a 70 by 5 uniform mesh of 9/3 elements. For the structure, a 60 by 2 uniform mesh consisting of 9-node elements was employed. Small displacements for the structure were assumed. The trapezoidal rule was employed in the time integration of the structural as well as the fluid flow equations.

In figure 6-5, the displacement history of the mid-point of the collapsible segment is shown. The segment moves downward and then begins to oscillate with increasing amplitude. Finally, a state is reached in which the amplitude of the oscillation remains constant, and the maximum downward displacement of the channel is closed to about 15 percent of its original height. A similar behavior was observed in experiments with excised blood vessels and rubber tubes (see for example [33]), and was also reported in numerical simulations [34], [35]. In figure 6-5, a comparison of the solution obtained using the proposed scheme and ADINA is also shown. The ADINA solution was obtained using a uniform mesh of 2800 (140 by 10) 3-node triangular elements with bubbles for the fluid and a 50 by 2 uniform mesh of 9-node elements for the structure. It is seen that the calculated responses are in good agreement.

The details of the pressure and velocity distributions at the time 36 sec., at which the collapsible segment becomes unstable, is shown in figure 6-6. Note that the

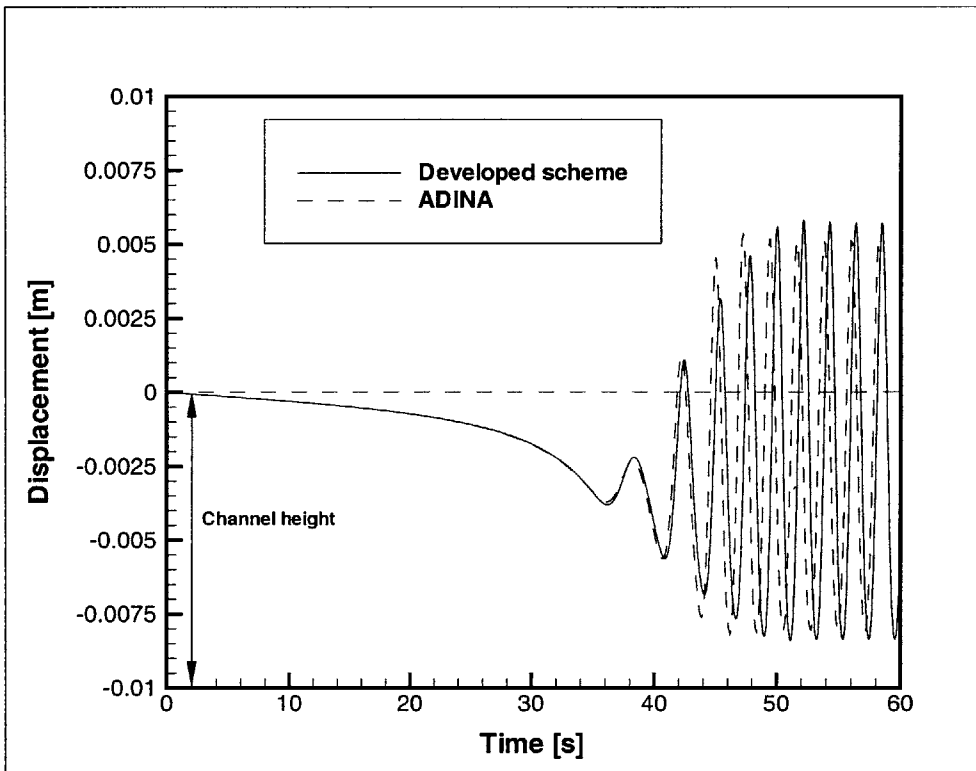


Figure 6-5: Displacement history of mid-point of collapsible segment. Comparison between results obtained using the proposed scheme and ADINA.

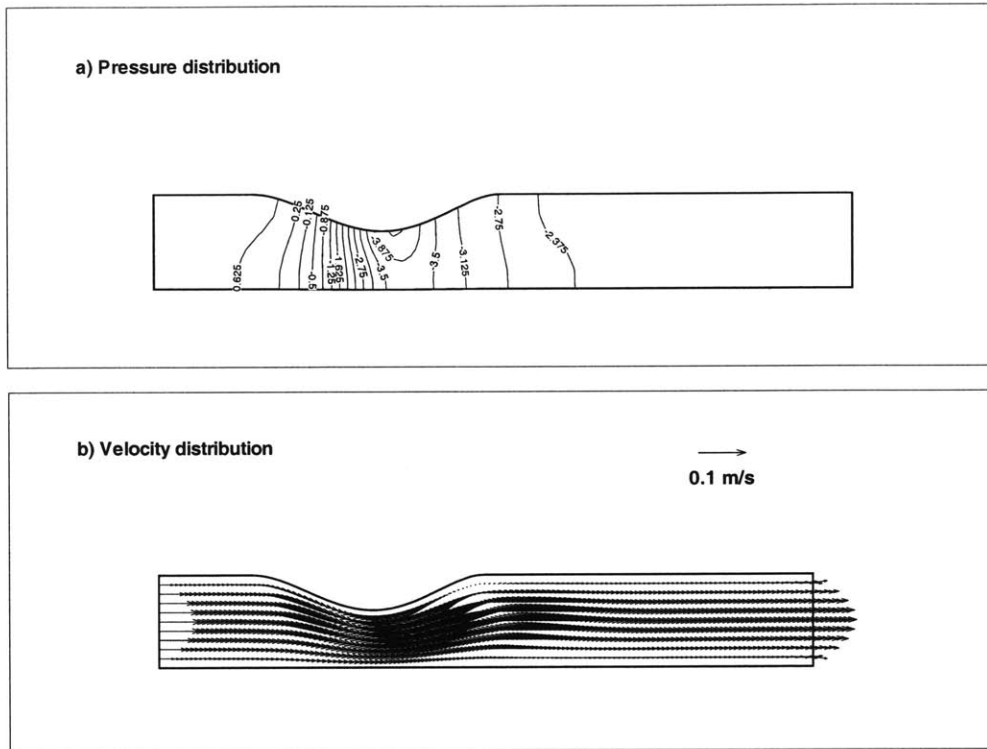


Figure 6-6: Pressure (in Pa) and velocity distribution of the fluid inside the collapsible channel at $t=36.2$ sec.

minimum pressure of the system is located below the collapsible segment.

Details of the pressure and velocity distributions at the maximum bulge out and maximum inward deflection of the collapsible segment are shown in figures 6-7 and 6-8, respectively.

If the collapsible channel problem is solved using partitioned procedures, a large number of iterations is required at each time step for convergence, and therefore partitioned procedures are inefficient for this particular case. Using the proposed scheme the iterations required to solve the problem are at least an order of magnitude less than with the partitioned procedure described in section 4.2.2.

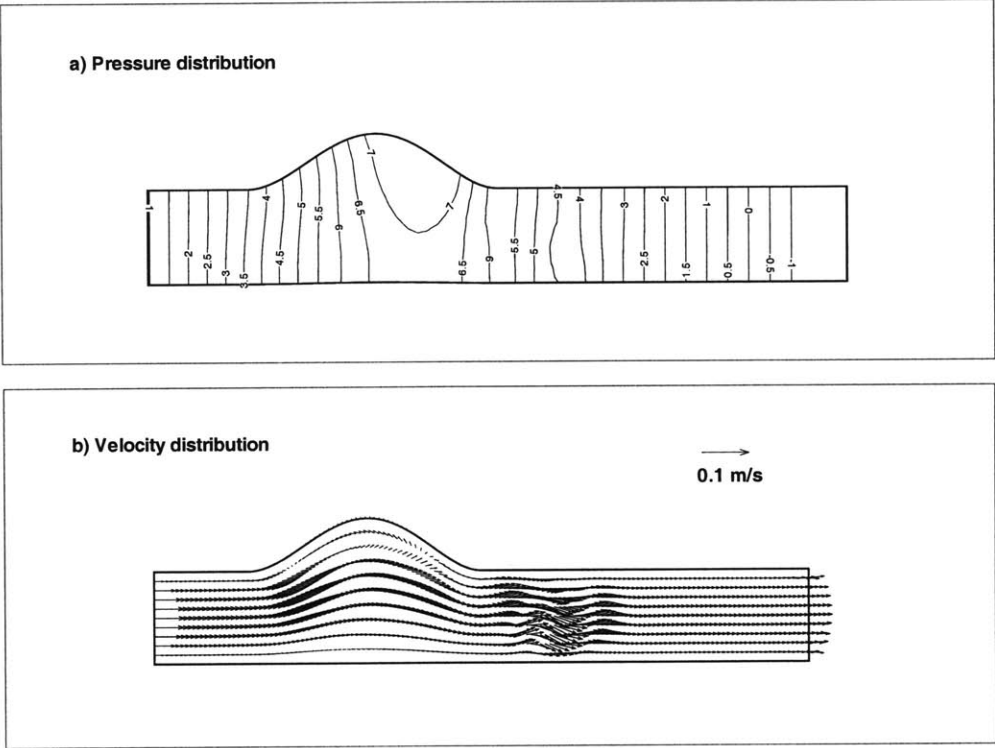


Figure 6-7: Pressure (in Pa) and velocity distributions at maximum bulge out of collapsible segment (when the movement reaches the limit cycle) at $t = 62.7$ sec.

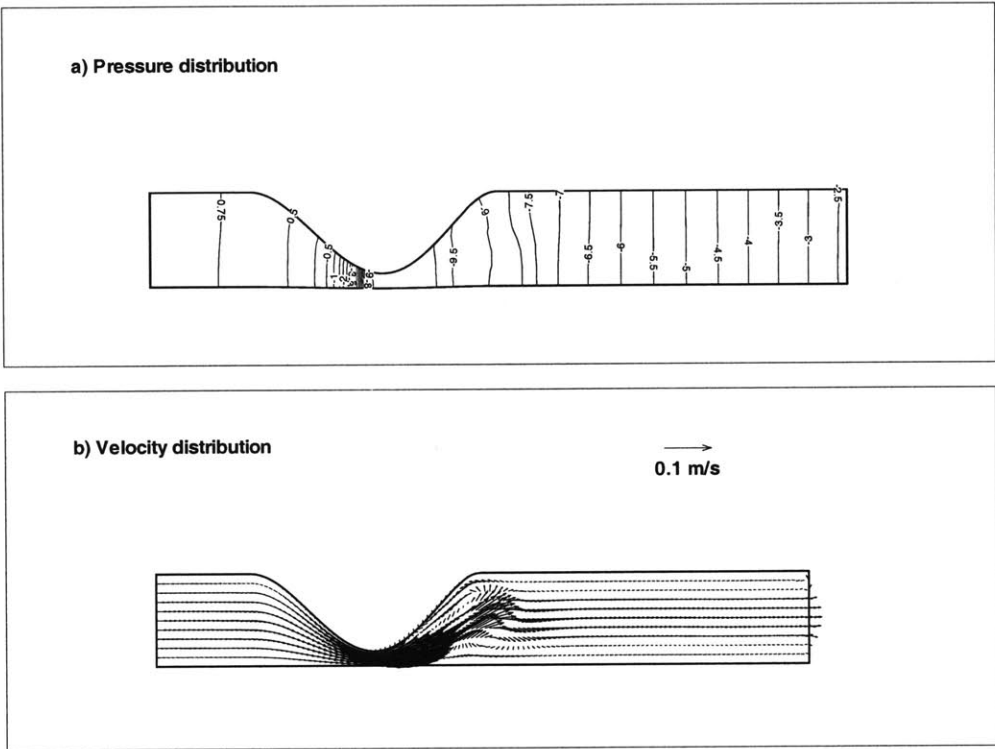


Figure 6-8: Pressure (in Pa) and velocity distributions at maximum inward deflection of the collapsible segment (when the movement reaches the limit cycle) at $t = 61.7$ sec.

Chapter 7

Conclusions

To numerically solve fluid flow-structural interaction problems, two main approaches are available. The simultaneous solution procedure can be unconditionally stable (if appropriate time integration schemes are used) but since the fluid flow equations are nonlinear and the resulting finite element coefficient matrix is non-symmetric, the cost of the computations dramatically increases with the degrees of freedom considered. Partitioned procedures have the advantage that the fluid flow and structural equations are solved separately and are coupled through “boundary conditions” at the fluid structure interface. This allows to solve larger problems than using the simultaneous solution, but a large number of iterations may be required to converge when the structure is very compliant.

In this thesis a procedure to solve fully coupled fluid flow-structural interaction problems is proposed. The scheme is in essence a simultaneous solution procedure and therefore has the same accuracy and stability characteristics. However, the scheme is computationally efficient (in terms of number of operations performed per time step) when the structure is compliant and in particular when the structural behavior can be assumed to be linear.

In the proposed scheme, the coupled system equations are not solved all together, but first the unknowns corresponding to the fluid flow equations containing the effects of the structure are solved, and then the unknowns corresponding to the structural equations are calculated. This approach is modular with respect to the fluid and

structural solvers used and allows the solution of large problems. The algorithm is computationally efficient since advantage can be taken of the symmetry of the structural coefficient matrix and, if applicable, the linearity of the structural equations. Since the proposed scheme is equivalent to the simultaneous solution procedure, iterations are required only for the nonlinearities in the problem, and no extra iterations are needed as in the case of partitioned procedures (where we need iterations between the structural and fluid solutions to converge the coupled problem). Hence when the structure is very compliant the computational costs can be greatly reduced.

The proposed scheme was implemented in a computer program and some problems were solved. The examples considered in this thesis (shown in chapter 6) correspond to problems in which the structure is very compliant. If the problems are solved using the partitioned procedure, significantly more iterations are required at each time step to converge to the solution as compared with the proposed scheme.

However, in the evaluation of the proposed scheme it has to be taken into account that the bandwidth of the coefficient matrix corresponding to the fluid flow equations with condensed internal structural degrees of freedom is increased as compared with the fluid flow equations alone (as solved by a partitioned procedure). Also, in practice, usually more degrees of freedom are required to accurately solve for the fluid flow response as compared with the structural response (in the coupled problem). Then, if the number of structural degrees of freedom is negligible in comparison with the number of fluid degrees of freedom, it becomes more convenient to solve the coupled equations using directly the simultaneous solution procedure (or a partitioned procedure if the effect of the coupling on the system response is not significant). In cases in which the structure is not very compliant, the partitioned procedure is more efficient, because then only a few iterations between the fields are required.

In summary, the proposed scheme is more efficient than both the simultaneous solution and partitioned procedures if the following conditions are satisfied,

- the structure is very compliant;
- the number of structural degrees of freedom in the coupled problem is significant;

- the structural behavior can be assumed to be linear.

The last condition, however, can be relaxed, and the proposed scheme might also be efficient when the structure exhibits a nonlinear response. In this case, we can still take advantage of the symmetry of the structural equations and the modularity of the proposed algorithm.

Appendix A

Wave propagation in a compliant tube filled with fluid

The problem considered here corresponds to the pressure propagation problem shown in figure (6-1). A simple analytical model, which yields results in good agreement with the numerical results obtained is given below.

Assume that an incompressible inviscid fluid fills the flexible axisymmetric tube of figure (6-1). Then the governing equations for the fluid are

- Mass conservation:

$$A_t + u A_x + A u_x = 0 \quad (\text{A.1})$$

- Momentum conservation:

$$u_t + u u_x + \frac{p_x}{\rho} = 0 \quad (\text{A.2})$$

where A is the tube transverse area, u is the fluid flow velocity in the axial direction (averaged over the transverse area), ρ is the fluid density, p is the pressure, t is time and the x coordinate is along the tube axis.

Assuming a constitutive relation of the form

$$p = P(A) \tag{A.3}$$

the pressure is considered to be a function of the transverse tube area alone (and therefore axial effects are neglected).

Considering small changes in the transverse area, $A/A_o \ll 1$, and assuming that the fluid velocity is much smaller than the wave speed c in the fluid, $u \ll c$, equations (A.1) and (A.2) can be linearized

$$A_t + A_o u_x = 0 \tag{A.4}$$

$$u_t + \frac{p_x}{\rho} = 0 \tag{A.5}$$

Solving for u in equation (A.5), substituting into (A.4) and differentiating with respect to time we get

$$A_{tt} = \frac{A_o}{\rho} p_{xx} \tag{A.6}$$

Also, from equation (A.3) we have

$$p_t = \frac{dP}{dA} A_t \tag{A.7}$$

and

$$p_{tt} = \frac{dP}{dA} A_{tt} \tag{A.8}$$

where the relation (A.8) was obtained after linearization.

Introducing equation (A.8) into (A.6), a linearized wave propagation equation is obtained

$$p_{tt} = \frac{A_o}{\rho} \frac{dP}{dA} p_{xx} \tag{A.9}$$

From equation (A.9) we have that the linearized wave speed c_o is given by

$$c_o^2 = \frac{A_o dP}{\rho dA} \quad (\text{A.10})$$

In order to evaluate the wave speed c_o we need an expression for dP/dA . The expression can be obtained by taking into account the behavior of the tube.

Assuming that the tube is made of a linear elastic isotropic material undergoing small displacements and neglecting axial and inertial effects, we obtain

$$\sigma_{\theta\theta} = E \varepsilon_{\theta\theta} \quad (\text{A.11})$$

and

$$\varepsilon_{\theta\theta} = \frac{\Delta R}{R_o} \quad (\text{A.12})$$

$$\sigma_{\theta\theta} = \frac{R_o \Delta p}{h} \quad (\text{A.13})$$

where $\sigma_{\theta\theta}$ and $\varepsilon_{\theta\theta}$ are the tube stress and strain components in the circumferential direction, E is the material Young's modulus, R_o is the undeformed tube radius and ΔR the change in the tube radius, Δp is the increase in pressure inside the tube (imposed by the fluid) and h is the tube thickness.

Combining equations (A.11), (A.12) and (A.13)

$$\frac{\Delta p}{\Delta R} \sim \frac{dp}{dR} = \frac{E h}{R_o^2} \quad (\text{A.14})$$

Then, introducing equation (A.14) into (A.10) the Moens-Korteweg wave speed is obtained

$$c_o^2 = \frac{E h}{2 \rho R_o} \quad (\text{A.15})$$

Bibliography

- [1] L. G. Olson and K. J. Bathe. Analysis of fluid-structure interactions. A direct symmetric coupled formulation based on a fluid velocity potential. *Computers & Structures*, 21:21–32, 1985.
- [2] K. J. Bathe. *Finite Element Procedures*. Prentice Hall, 1996.
- [3] H. J. P. Morand and R. Ohayon. *Fluid structure interaction: applied numerical methods*. John Wiley & Sons, 1995.
- [4] K. C. Park, C. A. Felippa, and J. A. DeRuntz. Stabilization of staggered solution procedures for fluid-structure interaction analysis. In *Computational methods for fluid-structure interaction problems*, number 26 in ASME Applied mechanics symposia series, AMD, pages 95–124, 1977.
- [5] K. J. Bathe, H. Zhang, and M. H. Wang. Finite element analysis of incompressible and compressible fluid flows with free surfaces and structural interactions. *Computers & Structures*, 56:193–213, 1995.
- [6] K. J. Bathe, H. Zhang, and X. Zhang. Some advances in the analysis of fluid flows. *Computers & Structures*, 64:909–930, 1997.
- [7] K. J. Bathe, H. Zhang, and S. Ji. Finite element analysis of fluid flows fully coupled with structural interactions. *Computers & Structures*, 1999. In press.
- [8] K. C. Park. Partitioned transient analysis procedures for coupled-field problems: stability analysis. *Journal of Applied Mechanics*, 47:370–376, 1980.

- [9] K. C. Park and C. A. Felippa. Partitioned transient analysis procedures for coupled-field problems: accuracy analysis. *Journal of Applied Mechanics*, 47:919–926, 1980.
- [10] S. Piperno, C. Farhat, and B. Larrouturou. Partitioned procedures for the transient solution of coupled aeroelastic problems. Part I: Model problem, theory and two-dimensional application. *Computer Methods in Applied Mechanics and Engineering*, 124:79–112, 1995.
- [11] C. Farhat, M. Lesoinne, and N. Maman. Mixed explicit/implicit time integration of coupled aeroelastic problems: three-field formulation, geometric conservation and distributed solution. *International Journal for Numerical Methods in Fluids*, 21:807–835, 1995.
- [12] W. A. Wall and E. Ramm. Fluid-structure interaction based upon a stabilized (ALE) finite element method. In *Computational Mechanics, Proceedings WCCM IV Conference*, Buenos Aires, 1998.
- [13] K. J. Bathe and E. L. Wilson. NONSAP - a general finite element program for nonlinear dynamic analysis of complex structures. In *Paper No. M3-1, Proceedings, Second Conference on Structural Mechanics in Reactor Technology*, Berlin, 1973.
- [14] T. Nomura and T. J. R Hughes. An arbitrary Lagrangian-Eulerian finite element method for interaction of fluid and a rigid body. *Computer Methods in Applied Mechanics and Engineering*, 95:115–138, 1992.
- [15] T. Nomura. ALE finite element computations of fluid-structure interaction problems. *Computer Methods in Applied Mechanics and Engineering*, 112:291–308, 1994.
- [16] C. Nitikitpaiboon and K. J. Bathe. An arbitrary Lagrangian-Eulerian velocity potential formulation for fluid-structure interaction. *Computers & Structures*, 47:871–891, 1993.

- [17] O. Ghattas and X. Li. A variational finite element method for stationary non-linear fluid-solid interaction. *Journal of Computational Physics*, 121:347–356, 1995.
- [18] S. J. Liang, G. P. Neitzel, and C. K. Aidun. Finite element computations for unsteady fluid and elastic membrane interaction problems. *International Journal for Numerical Methods in Fluids*, 24:1091–1110, 1997.
- [19] L. E. Malvern. *Introduction to the mechanics of a continuous medium*. Prentice-Hall, 1969.
- [20] F. M. White. *Fluid mechanics*. McGraw-Hill, 1979.
- [21] J. Donea. Arbitrary Lagrangian-Eulerian finite element methods. In T. Belytschko and T. J. R. Hughes, editors, *Computational methods for transient analysis*, chapter 10. North-Holland, 1983.
- [22] M. D. Gunzburger. *Finite element methods for viscous incompressible flows. A guide to theory, practice and algorithms*. Academic Press, Inc., 1989.
- [23] A. N. Brooks and T. J. R. Hughes. Streamline upwind/Petrov-Galerkin formulations for convection dominated flows with particular emphasis on the incompressible Navier-Stokes equations. *Computer Methods in Applied Mechanics and Engineering*, 32:199–259, 1982.
- [24] D. Hendriana. *A parabolic quadrilateral finite element for compressible and incompressible flows*. PhD thesis, MIT, 1998.
- [25] D. Hendriana and K. J. Bathe. On a parabolic quadrilateral finite element for compressible flows. *Computer Methods in Applied Mechanics and Engineering*, 1999. In press.
- [26] X. Wang. *On mixed finite element formulations for fluid-structure interactions*. PhD thesis, MIT, 1995.

- [27] C. Nitikitpaiboon. *Finite element formulations for fluid-structure interaction*. PhD thesis, MIT, 1993.
- [28] C. A. Felippa and K. C. Park. Staggered transient analysis procedures for coupled mechanical systems: formulation. *Computer Methods in Applied Mechanics and Engineering*, 24:61–111, 1980.
- [29] T. J. R. Hughes. Analysis of transient algorithms with particular reference to stability behavior. In T. Belytschko and T. J. R. Hughes, editors, *Computational methods for transient analysis*, chapter 2. North-Holland, 1983.
- [30] C. W. Gear. *Numerical initial value problems in ordinary differential equations*. Prentice-Hall, 1971.
- [31] K. Ogata. *Modern control engineering*. Prentice Hall, 1997.
- [32] M. Bathe and R. D. Kamm. A fluid-structure interaction finite element analysis of pulsatile blood flow through a compliant stenotic artery. *ASME, Journal of Biomechanical Engineering*, 1999. In press.
- [33] T. J. Pedley. *The fluid mechanics of large blood vessels*. Cambridge University Press, 1980.
- [34] X. Y. Luo and T. J. Pedley. A numerical simulation of unsteady flow in a two-dimensional collapsible channel. *Journal of Fluid Mechanics*, 314:191–225, 1996.
- [35] C. Walsh, J. S. Hansen, and P. A. Sullivan. Effects of axial tension and downstream suction on flutter in membrane-walled collapsible tubes. In *Advances in Bioengineering*, number 20 in ASME - BED, 1991.

6716-35